

Guidelines for Avoiding Vortex Wakes During Use of Closely-Spaced Parallel Runways

Vernon J. Rossow* and Larry A. Meyn†

NASA Ames Research Center, Moffett Field, CA 94035

This paper proposes a reliable method for estimation of the movement and spread of lift-generated vortex wakes as a function of time to better enable aircraft arriving at airports to avoid the hazards associated with the wakes of preceding aircraft. Operations on closely-spaced parallel runways illustrate how the method may be applied. An overview presents the aerodynamic mechanisms that cause the hazardous parts of lift-generated wakes to spread as a function of time. A computational method developed for determination of the spread of vortex wakes as a function of time is then applied to operations of aircraft as they approach closely-spaced parallel runways. The results suggest guidelines for efficiently and effectively avoiding the vortex wakes of preceding aircraft. Because the theoretical tools developed and the measurements of the components of the time-averaged wind and its gust magnitudes contain uncertainties, flight tests are recommended to confirm and to refine the guidelines presented, and to verify the techniques used to measure the atmospheric parameters that control wake intrusion.

Nomenclature

| | |
|------------|--|
| a | = peak-to-peak amplitude of long-wave instability, ft (m) |
| A | = a/b_g |
| b | = wingspan, ft (m) |
| b' | = span wise distance between vortex centers $\approx \pi b_g/4$, ft (m) |
| B_{hz} | = breadth of hazardous part of wake region to be avoided, ft (m) |
| C_L | = lift coefficient = Lift/ $q_\infty S$ |
| C_l | = rolling moment coefficient = Rolling moment/ $q_\infty S b$ |
| D_{hz} | = depth of hazardous part of wake region to be avoided, ft (m) |
| GPS | = global positioning system |
| Kn | = knots |
| G | = $\Gamma/b_g U_\infty$ |
| q_∞ | = $\rho_\infty U_\infty^2/2$ |
| S | = planform area of wing, ft ² (m ²) |
| t | = time, s |
| T_g | = τG |

* Ames Associate, Aviation Systems Division, Mail Stop 210-10, AIAA Associate Fellow.

† Aerospace Engineer, Aerospace Operations Modeling Branch, Mail Stop 210-10, AIAA Associate Fellow.

x = distance in flight or longitudinal direction, ft (m)
 y, z = distance in lateral and vertical directions, ft (m)
 u, v, w = velocity components in x, y and z directions, ft/s (m/s)
 U_∞ = velocity of wake-generating aircraft, ft/s (m/s)
 Wt = weight, lbs (N)
 Δt = time interval between wake-generating and following aircraft
 ϵ = turbulence level or eddy-dissipation rate
 Γ = centerline circulation on wing, ft²/s (m²/s)
 θ = angle between vertical and plane of waves, degrees
 ρ = air density, slugs/ft³ (kg/m³)
 τ = time parameter = tU_∞/b_g

Subscripts

0 = initial value
 decomp = decomposing wake
 eff = effective
 f = following aircraft
 fil = vortex filament
 g = wake-generating or leading aircraft
 grdef = ground effect
 Lnk = linking of vortex pair
 lw = long-wave instability of vortex pair
 max = maximum
 min = minimum
 ops = operations
 oval = streamline oval that encloses vortex pair
 pln = plan view
 pr = vortex pair
 rnwy = runway
 spread = wake-spreading amount
 t = turbulence
 wnd = wind
 ∞ = free-stream condition

I. Introduction

A. Background.

If the lift-generated wakes of aircraft were not hazardous, and did not persist for several minutes, runways could be safely located close each other and re-used within time intervals based only on air-traffic management constraints rather than on aerodynamic ones that relate to flight safety.¹ Because lift-generated wakes of aircraft pose a hazard, studies have been conducted on ways to reduce the effect of vortex wakes on airport capacity. One such method considered the transport and decay of vortex wakes as a function of time as a means to shorten the time required for single runways to become vortex free for re-use.²⁻¹¹ It was found that the capacity of a single runway might then be increased by as much as 10% by judicious use of weather information and aircraft timing. Although beneficial, such an improvement does not accommodate the factor of two or three increase in traffic volume that is expected during the next 20 years. It was therefore reasoned that improvements in the use of a single runway would not achieve the desired goal, and that the number of runways at each airport will need to be increased. An increase in the number of runways at most airports is not possible if the runways are built with conventional lateral spacings of 4300 ft (or 1311 m) so that they can be operated independently. Because available land area at or near existing airports is already in short supply, current research has focused on the use and addition of closely-spaced parallel runways, which are often spaced parallel to each other at distances of 750 ft (or 230 m) or more. The runways are then too close to operate independently, because wakes of preceding aircraft might intrude into the air space of a following aircraft. Management of aircraft flight paths will then require more planning due to proximity of aircraft to one another, and due to the higher density of aircraft traffic in the air and on the ground.

The research reported addresses the development of a reliable method for estimation of the rate at which lift-generated vortex wakes of subsonic transport aircraft move and spread due to the wind and turbulence in the atmosphere along the flight path of arriving aircraft, and due to self-induced spreading mechanisms by the vortex wake. Previous studies have examined the details of various aerodynamic mechanisms that cause the vortex wakes of subsonic aircraft to spread and to move.¹²⁻²⁰ This paper first presents an overview of the results of the research conducted on the wake-spreading and movement mechanisms that influence the time at which intrusion of wake components into the airspace of following aircraft will occur. Estimates carried out by use of a computer program based on previous studies (see Appendix) indicate guidelines that may be used to expedite the volume of aircraft operations safely and efficiently onto closely-spaced parallel runways. The results indicate that aircraft pairs landing on two parallel runways need not do so in a side-by-side operation, but that their along-trail spacing may be safely increased to 10 s or more. The reliability of the estimate and the magnitude of the time increment are enhanced if smaller aircraft are used as the leading aircraft and if following aircraft land upwind of leading aircraft when a side wind is present. Suggestions for aircraft-management systems at airports that might help to provide the guidance and timing of aircraft necessary for higher capacity (and for higher density of aircraft) at airports, and their control on approach and departure are treated elsewhere.²¹⁻³³

B. Application to Closely-Spaced Parallel Runways.

Although the results provided here on the movement and spread of vortex wakes has application to a variety of wake-vortex situations, the results are applied here to approach and landing operations on closely-spaced parallel runways. Therefore, the first part of the airport-capacity problem is one of intrusion of the vortex wakes shed by a leading aircraft into the airspace of a following aircraft. The wake-decomposition part of the capacity problem is assumed to not be appreciably changed if recycle times are based on the arrival of the following aircraft.

The use of closely-spaced parallel runways is not new. At present, operations are conducted as nearly simultaneous landings during visual meteorological conditions (VMC). Encounters with vortex wakes are then safely avoided because the along-trail spacing between aircraft landing on two closely-spaced parallel runways is so small that the vortex wake shed by either aircraft does not have time to spread enough to intrude into the airspace of the other aircraft, until after both have landed (Fig. 1). Therefore, an aerodynamic avoidance problem has been solved for simultaneous operations of arriving aircraft.

When the weather or visibility degrade runway operations to instrument conditions (IMC), only one of the two closely-spaced parallel runways is used, which cuts the landing capacity in half and reduces the capacity of the two runways to single-runway operation. Efforts have been underway for some time to enable two aircraft to safely conduct nearly simultaneous landings during IMC so that operations can be carried out continuously. Research with piloted simulators, however, has shown that along-trail time intervals between aircraft in a pair should be increased to five s or more³¹ when pilots need to rely totally on electronic guidance and location of nearby aircraft. Also, because it is often not possible to form pairs of aircraft that have the same approach and landing velocities, along-trail distances might vary much more than about 5 s. These and other conditions may make it difficult for the following aircraft to stay within the safe zone behind the leading aircraft. When this occurs, the following aircraft must wait until the vortex wake of the lead aircraft has decomposed to a non-hazardous level, which also reduces the capacity of the two runways to that of single-runway operations. For the foregoing reasons, and others that may arise, it is highly desirable that the estimated size of the safe zone indicated in Fig. 1 be as large as possible. If this is to be done safely, the theoretical estimates of wake movement and spreading must be reliable, with few if any uncertainties.

The prediction of wake-spreading as a function of time, and the way that atmospheric conditions affect this aerodynamic problem¹²⁻²⁰ are first summarized in order to develop a reliable computational method for prediction of the duration of the safe zone illustrated in Fig. 1. The results presented assume that the transition from a VMC to an IMC capability at airports has been completed.²¹⁻³³ For a number of operational reasons, success with wake-avoidance technologies will have been achieved when the safe zone for the along-trail separation distance, or time between the two aircraft, can be safely increased from nearly simultaneous (or 5 s, i.e., about

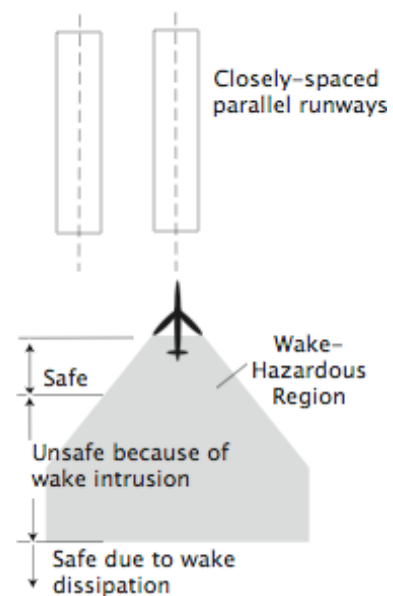


Fig. 1 Safe and unsafe along-trail separation distances for following aircraft due to intrusion of wake shed by leading aircraft into its airspace.

1000 ft or 305 m) to as much as 10 s (about 2000 ft or 610 m) or more. The larger along-trail separation distances facilitate wave-off operations and accommodate required aircraft-grouping combinations. Estimates carried out by use of a computer program presented in the Appendix indicate that the safe zone associated with side-by-side approaches can usually be safely increased to 10 s or more, if the smaller aircraft in the pair is the leading aircraft and if the following aircraft lands upwind of the leading aircraft when a side wind is present.

II. Movement and Spread of Wake-Hazardous Regions

Wake-intrusion time depicted in Fig. 1 depends on the lateral separation distance between the runways, the sizes of the aircraft, the time-averaged wind magnitude and direction, and the turbulence magnitude in the atmosphere where the wake of the generating aircraft is deposited. As mentioned in the introduction, the lateral extent and location of wake-hazardous regions is studied because the altitudes of the two aircraft on approach to a set of parallel runways will usually be close to the same at a given station along their approach paths, thereby reducing the problem to a lateral one. Only an overview of previous results is presented here because considerable attention has already been given to the details of the aerodynamics of how vortices move and spread.¹²⁻²⁰ In this work, the movement and spread of lift-generated vortex wakes by aerodynamic means has been divided into the following mechanisms:

- A. Size of wake-hazardous region around initial location of vortex pair.
- B. Spread of wake-hazardous region by turbulence.
- C. Wake spreading by long-wave instability.
- D. Self-induced downward and lateral movement of vortex pair.
- E. Long-term self-induced spreading by turbulence.
- F. Movement of wake-hazardous boundaries by wind and gusts.

Any deviations by the wake-generating aircraft in a vertical or horizontal direction from the intended flight path are assumed to be small enough that they have a negligible effect on wake spreading, and are therefore not included in the computations.

A. Size of Wake-Hazardous Region Around Vortex Pair.

The center of a vortex shed by a preceding aircraft is the most hazardous location for an encounter. As indicated in Fig. 2, the hazard extends with decreasing intensity for some distance away from the center of each of the two vortices in the pair. A wake-hazardous region is therefore defined as that part of the atmosphere that must be avoided by following aircraft, because hazardous elements of a lift-generated vortex pair shed by a preceding aircraft, and the hazard they pose, are located therein to within a high degree of certainty.³⁴⁻³⁷ The term wake-hazardous region is used to describe the region to be avoided because, if the centerline of a following aircraft is outside of the boundary of a given hazardous region, any disturbances induced on a following aircraft by the vortex wake of a preceding aircraft is indistinguishable from an encounter with ambient turbulence in the area.

Because the vortex-induced rolling moment fades approximately as the square of the distance from the center of the wake, the choice of a maximum tolerable vortex-induced rolling moment is somewhat arbitrary.^{1,34} The present study uses the specification that the centerline of the following aircraft must be far enough from the centerline of the wake generated by a preceding aircraft so that it does not encounter a vortex-induced rolling moment larger than one-sixth of the roll-control authority available by use of the ailerons. This definition is based on simulated encounters with vortex wakes which indicate that the following aircraft will not roll more than 5° if the vortex-induced rolling moment is less than one-half of the roll-control authority on the aircraft.³⁴ The one-sixth value is used instead of the one-half value, because it is more conservative and does not greatly increase the size of the region to be avoided.

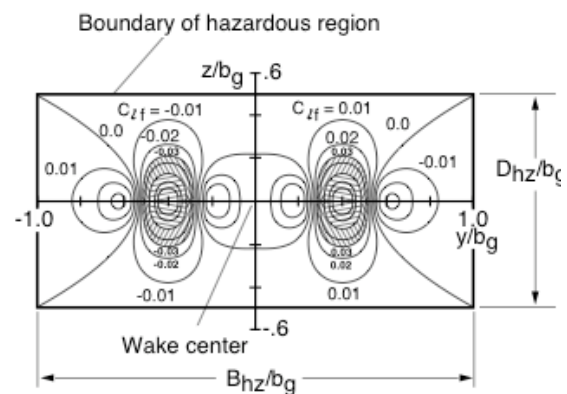


Fig. 2 Contours of constant wake-induced rolling moment coefficient used to define initial boundaries of hazardous region; $C_{Lg} = 1.5$, $b_f/b_g = 0.29$, maximum $C_{Lf_{max}} = 0.12$.

The contours of equal vortex-induced rolling moment shown in Fig. 2 were calculated theoretically and confirmed by wind-tunnel experiments.³⁴⁻³⁷ The calculations carried out to generate Fig. 2 assume that the flow field in which the vortices are embedded is steady with time (i.e., no wind or turbulence). The contours shown are based on a combination of theory and experimental confirmation at a time, or short distance, behind the wake-generating aircraft where the wake can be considered to be rolled up. When the vortex sheet shed by the wing has rolled up, the vortex wake, and the hazard that it causes, is noted to extend out beyond the wing tips of the wake-generating aircraft. Lines of constant vortex-induced rolling-moment coefficient then have a well-defined structure that changes slowly with time. The centers of the vortex pair that drive the velocity distribution in the wake remain in about the same relative location until three-dimensional disturbances begin the process of wake decomposition. Before that time, the contours of constant rolling-moment coefficient shown in Fig. 2 approximate the steady-state, or time-averaged, values that would be experienced by aircraft in an actual flight situation.

At aircraft span ratios larger than $b_f/b_g = 0.29$, the dimensionless size of a box that encloses the 0.01 rolling-moment contours is roughly constant until the span ratio exceeds 0.5. For example, when the span ratio is equal to 1.0, computed contours of equal rolling moment, like those shown in Fig. 2, indicate that the size of the hazardous region is about $2.5 b_g$ in breadth and b_g in depth.^{13,34} To have a continuous relationship for the initial size of the hazardous region as a function of span ratio, the span-wise breadth is approximated by $B_{hz0} \approx 2 b_g$ when $b_f/b_g < 0.5$. When $b_f/b_g \geq 0.5$, the breadth of the hazardous region is approximated by

$$B_{hz0} \approx [2 + (b_f/b_g - 0.5)] b_g \quad (1)$$

The initial depth of the hazardous region, $D_{hz}(t)$, is roughly constant at one span, independent of span ratio. The initial hazardous region is, of course, centered on the centerline of the wake-generating aircraft at the time that it is generated, but rapidly becomes offset laterally due to the steady-state component of the ambient wind, and vertically due to the self-induced downward motion of the wake,

$$w_{pr} = -|\Gamma_{ac}|/2\pi b' \quad (2)$$

where, w_{pr} is the initial value of the self-induced velocity of the vortex pair, Γ_{ac} is the centerline circulation bound in the wing of the wake-generating aircraft, which is equal to the circulation content of each of the two vortices in the pair, and b' is the span-wise distance between the centroids of circulation for the two vortices in the pair.

B. Spread of Wake-Hazardous Region by Turbulence.

When vortex wakes are embedded in a quiescent fluid, like a water tow tank, the vortices remain relatively straight and decompose slowly. The two vortices then begin their trails as straight lines from near the wingtip regions at about $y/b_g = \pm\pi/8$, as indicated by the straight lines labeled as “Undisturbed vortices” in Fig. 3. As described in the previous section, the initial breadth of the wake-hazardous region is $B_{hz}(0) = 2b_g$, when, $b_f/b_g \leq 0.5$. The sides of the hazardous region are labeled as “Initial sides of the hazardous region” in Fig. 3. The other lines in the figure indicate the outboard boundaries of the hazardous region due to contributions directly or indirectly related to the turbulence in the air where the vortices are embedded. A turbulent flow field is defined as one wherein the flow field has

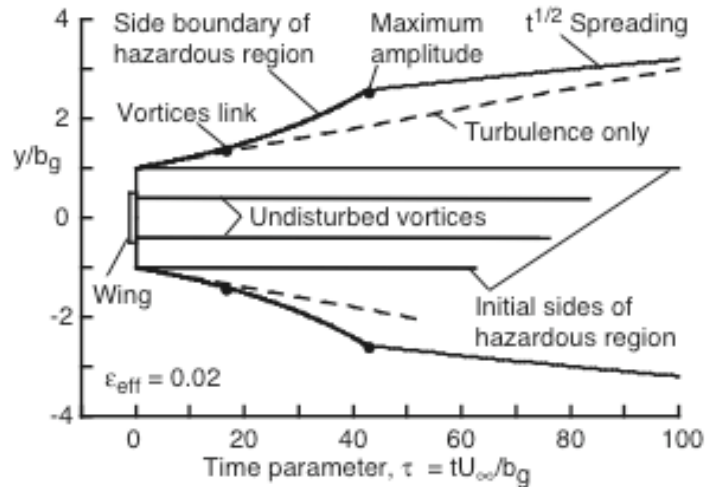


Fig. 3 Plan view of contributions to spread of wake-hazardous region as a function of time/distance behind generating wing; $b_f/b_g \leq 0.5$.

random unsteady motions superimposed on its time-averaged orderly motion.³⁸ The unsteady-random motions are eddies or swirling motions whose sizes vary from smaller than the wing chord, up to a number of span lengths. The magnitude of these velocity perturbations relative to the flight velocity of the aircraft is usually small.

Three sources of turbulence are usually present in the region occupied by the vortices after being shed by the lifting surfaces on a wake-generating aircraft. The first source is from the atmosphere through which the aircraft is flying. The turbulence from the second source is placed in the wakes of aircraft by the aircraft itself, which includes its various lifting surfaces. The sizes of the eddies generated on the surfaces of the airframe go from very small in the viscous boundary layer on the surface of the aircraft, to a fraction of a wingspan in regions of flow separation. Trailing vortices are coherent and organized in structure and so are not considered sources of turbulence, until the highly organized structure of vortex wakes begins to decompose and decay.

The third source of turbulence consists of flow disturbances generated by the energized streams from the propulsion system on board the wake-generating aircraft. Jet-induced disturbances usually go directly into the region occupied by the rolled-up vortices, and can therefore be an important source for disturbances that are able to modify the structure of vortices shed by the wing. Immediately behind the aircraft, the jet structures consist of highly energized cores with sharply defined cylindrical shear layers surrounding them. About one span behind the aircraft, the jet streams begin to break up into turbulent eddies that grow from quite small at jet exits, into eddies that are about the size of the wingspan of the aircraft, or larger. As the dominant eddies grow in size, their swirl velocities become smaller until the turbulence within the wake becomes dispersed over a large region that grows roughly as the square root of time.³⁹ Eventually, the velocity magnitudes in the wake become difficult to distinguish from those in nearby atmospheric turbulence.

The time-averaged magnitude of these unsteady random motions where the vortex wake is embedded is called the turbulence level of the fluid. The intensity of the turbulence is usually found by measurement of the magnitudes of the root-mean-squared value of the time-dependent velocity perturbations. The turbulence level of the flow field is then the ratio of such a measurement divided by a characteristic velocity of the steady motions. For example, in wind tunnels the turbulence level, ϵ_t , is given by³⁸

$$\epsilon_t = [(\bar{u}'^2 + \bar{v}'^2 + \bar{w}'^2) / 3U_\infty^2]^{1/2} \quad (3)$$

where the three primed and barred quantities inside the set of parentheses represent the time-averaged values of the square of the three components of the measured perturbation velocities in the air stream of the empty wind-tunnel. The quantity, U_∞ , is the time-averaged velocity of the air stream, which is in the x-direction and aligned with the centerline of the wind tunnel.^{40,41}

Of interest here is the fact that the turbulence in the air stream, no matter what the source, causes segments of vortex wakes to migrate randomly so as to spread wake segments, and their hazardous character, to locations outside of the initial boundaries of the wake-hazardous region. The time-averaged outer boundary of the spread of vortex centers with downstream distance is shown in plan view in Fig. 3 by the two dashed lines for a turbulence level of $\epsilon_t = 0.02$. The beginning point of the two dashed lines is noted to be at the maximum lateral location of the initial size of the wake-hazardous region, rather than at the span-wise location where the vortices originate. This relocation is done because any span-wise or lateral change in vortex location causes the outer boundary of the hazardous region to change as well. Because only the outer boundary of the wake-hazardous region is of interest, any increase in the lateral location of a vortex center must be added onto the maximum breadth of the hazardous region. It is thereby assumed that the structure of a vortex is largely unchanged by its movement. These two assumptions may be overly conservative.

Other than an intuitive realization that turbulence causes vortex elements to spread as a function of time, the only quantitative experimental evidence that vortices meander about due to turbulence is found in some wind-tunnel experiments.^{35,36} The purpose of the experiments was to obtain measurements of the structure of lift-generated vortex wakes of transport aircraft at various downstream distances behind the aircraft model. It was found that turbulence in the region where the vortices were embedded did slowly change the structure of the vortices, but the largest influence was that turbulence in the ambient stream caused an across-stream unsteady and random motion (or meander) of the vortex centers in the 40- by 80-Foot and 80- by 120-Foot Wind Tunnels at NASA Ames Research Center. The magnitude of the meander distance was found to increase linearly with downstream distance, and thereby spread the hazardous region of the wake at a linear rate.

Based on these wind-tunnel measurements, a value for a vortex-meander-based turbulence level can be evaluated as: $\epsilon_{\text{meand}} = |\bar{v}'|/U_\infty \approx |\bar{w}'|/U_\infty \approx 2/(12 \times 81) \approx 0.002$. Because both wind-tunnel facilities have a measured

turbulence level of about, $\epsilon_t = 0.005$,^{40,41} the maximum values of measured across-stream displacements of the vortex centers are only about 40% of the amount predicted by use of the across-stream time-averaged velocities in the turbulent flow field of the wind tunnel. Although ϵ_{meand} is of the same order of magnitude as the $\epsilon_t = 0.005$ level measured for the turbulence in the free stream, and maximum values of meander distance are less by a substantial amount, it is not clear how the difference between the two should be reconciled. It is suggested that the difference of the two quantities is brought about by the fact that the swirling velocity for a given eddy in the turbulent flow field does not remain constant but decreases rapidly with time. If true, the average velocity associated with a particular swirling element in the turbulent flow field could be considerably less than the time-averaged perturbation velocities. Whatever the reason for their difference, it is believed that an adjustment constant (i.e., $\epsilon_{\text{meand}}/\epsilon_t = 0.4$) for a relationship between the turbulence measured in the two large wind tunnels and the turbulence that causes meander should not be used at this time, because the measured differences are not understood, and because an assumption that maximum meander distances are given by

$$\epsilon_t \approx |v'|_{\text{max}}/U_\infty \approx |w'|_{\text{max}}/U_\infty \quad (4)$$

is more conservative. For this reason, both vortex-meander distances and initiation of the long-wave instability are based on Eq. (4). Therefore, for wake-spreading computations, it is assumed that $|v'|_{\text{max}}$ and $|w'|_{\text{max}}$ are the representative quantities for reliable (and conservative) predictions of the hazardous region of vortex wakes. Because the most rapid aerodynamic spreading mechanism is the long-wave instability of a vortex pair, the measurements should be taken at all wavelengths between about $2 b_g$ and $10 b_g$ by each wake-generating aircraft as it moves along its approach path to a landing.⁴²⁻⁴⁴ In this way, the worst case situation is used for both the size of the disturbance and the most effective wavelengths for initiation of the long-wave instability of a vortex pair.

Equation (4) is believed to be more conservative and reliable than some methods used previously to determine typical values for the disturbance velocities for motion of vortex structures.^{42,43,49} The earlier methods are based on the fact that the velocity disturbances in various turbulent flow fields tend to have common values for velocity and size that can be modeled by one of several turbulence spectrums. The spectrums relate the velocity field of the turbulence to the wavelength of the disturbance. Although the Kolmogorov turbulence spectrum has often been used to characterize turbulence velocity variations as a function of the wavelength of the disturbance for a number of time-dependent structures of vortex wakes, its use in the determination of the maximum values for the magnitude of disturbance velocities is believed to be less applicable than direct measurement of them along the flight path of the wake-generating aircraft. Here and in sections to follow, it will be assumed that the magnitude of disturbance velocities are found by use of measurement of the maximum values of disturbance velocities taken along the flight path of the wake-generating aircraft over the frequency range where the long-wave instability of Crow is readily initiated.

An equation for the broadening of the wake-hazardous region due to ambient turbulence, without the long-wave instability, is then written as

$$\Delta B_{\text{hzt}} = 2\epsilon_{\text{max}} U_\infty \Delta t \quad (5)$$

where, ΔB_{hzt} is the broadening of the initial wake-hazardous region as caused by turbulence, and, ϵ_t , is based on the largest values found for the across-wake perturbation velocities that bring about vortex meander. When vortex spreading is added to the initial breadth of the wake-hazardous region, the boundaries expand as a function of time or distance by the amounts shown by the two dashed lines labeled as “Turbulence only” in Fig. 3.

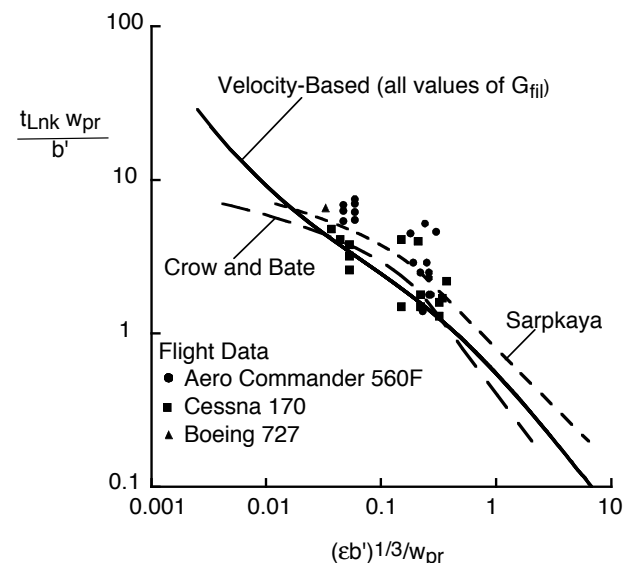


Fig. 4 Comparison of predicted linking times as a function of magnitude of disturbance velocity for long-wave instability of a vortex pair in terms of parameters used by Crow and Bate⁴² and by Sarpkaya.⁴⁹

C. Wake Spreading by Long-Wave Instability.

The long-wave instability of a vortex pair (or Crow instability) comes about when lateral and vertical local sinusoidally-shaped displacements are induced on the filaments by turbulence in the region of the atmosphere where the vortices are embedded. The instability has been studied extensively because it decomposes and spreads lift-generated vortex wakes more rapidly than any other known mechanism.^{16,20,42-49} If the vortex filaments are not disturbed from a straight-line configuration, the instability does not occur and the vortices trail from the wing as nearly straight lines (Fig. 3). However, because turbulence along the flight path of aircraft is usually present from one source or another, the vortices become sinuous and the instability occurs. The growth rate of the instability depends on the magnitude of the disturbance velocities in a direction across the vortex filaments, which is usually expressed as the intensity of the turbulence where the vortex is embedded (Fig. 4). If the turbulence level is low, it takes a long time for the vortices in the pair to link, and if the turbulence is intense, the growth rate of the instability is rapid.

The predictions of vortex linking times by three theories are presented in Fig. 4 along with data taken in flight tests.^{43,44} The data and the three theories are in fairly good agreement as plotted on the logarithmic scales used, but also indicate considerable scatter when put in terms of seconds, or distance, used during operations at airports. Some of the scatter in the flight data has been resolved by consideration of the amount of circulation contained in the filament, rather than the entire vortex, but additional parts of the deviations in the data are believed to be associated with the method that was used to measure wind velocity and atmospheric turbulence. It is believed that a satisfactory method has not yet been determined for measurement of the magnitude of the disturbance velocity parameter to be used in the prediction of wake intrusion into a nearby runway.²⁰

If the axes in Fig. 4 are linear and the dimensionless parameters used for the axes consist of parameters usually used during flight operations at airports, the predictions of vortex linking times appear as indicated in Fig. 5.^{16,20} The velocity-based growth-rate equation includes the possibility that the circulation content of the vortex filaments may not be the same as the estimate based on the maximum content possible just behind the wake-generating wing. The parameter G_{fil} in Fig. 5 covers such a possibility. The velocity-based analysis thereby allows the strength of the vortex pair to differ from the one estimated based on of an idealized wake with a single vortex pair. Observations of vortex wakes at cruise altitudes indicate that wakes often divide into several pairs and that the high-speed vortex core is the only part of the vortex wake that participates in the vortex-linking process. Therefore, multiple curves for the strength of the vortex pair going through the linking process are presented in Fig. 5.

The method used to compute the wake spreading caused by the long-wave instability has been studied in a previous paper,²⁰ and will therefore only be mentioned here. It is pointed out that wake spreading is a combination of the self-induced and turbulence-induced velocity contributions to the lateral spreading of the wake due to the long-wave instability. The differential equation is found by use of a combination of equations that describe those quantities as

$$dA_{pln} = [(dA_{lw}/d\tau)/2^{1/2} + 2\epsilon_{max}] d\tau \quad (6a)$$

The dimensionless plan-view amplitude of the waves induced on vortex filaments, A_{pln} , is a function of time, the circulation content of the vortex filaments, G_{fil} , and the maximum magnitude of turbulence disturbances, ϵ_{max} , in the atmosphere where the vortices are embedded. Eq. (6a) is therefore more complex than the solutions provided by Crow and Bate⁴³ and by Sarpkaya,⁴⁹ and must therefore be integrated numerically to determine a result.

The amplitude of the sinusoidal waves on vortex filaments during the early part of the instability have been observed to not be greatly enhanced by the self-

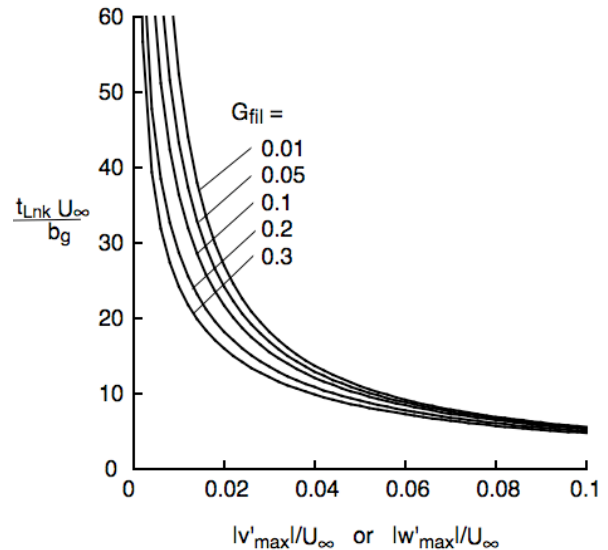


Fig. 5 Velocity-based estimate for linking time as a function of magnitude of disturbance velocity for long-wave instability of a vortex pair plotted on linear scales in terms of parameters recommended for applications.

induced velocity field of the long-wave instability until their amplitude exceeds the vortex-linking point.²⁰ As a result, the amount of wake spreading up to the linking point is approximated by the simple relationship provided by the turbulence-only curves in Fig. 3. The strong-turbulence form of the linking equations derived by Crow and Bate, and by the velocity-based analysis, can then be used to approximate the spreading of the hazard posed by vortex wakes during the early part of wave formation where turbulence dominates wake spreading, or

$$\tau_{Lnk} \approx (\pi/8)/\epsilon_{max} \approx 0.4/\epsilon_{max} \quad (6b)$$

where, $\tau_{Lnk} = t_{Lnk}U_\infty/b_g$ and it is assumed that $\epsilon_{max} \approx |v'_{max}| \approx |w'_{max}|$.

D. Self-Induced Downward and Lateral Movement of Vortex Pair.

It is assumed that the separation distance between the centroids of the port and starboard vortices is approximated by the value for elliptically-loaded wings as, $b' \approx \pi b_g/4$. The corresponding value for the self-induced downward velocity of the vortex pair (before wake decomposition begins and when far above the ground plane) is given by

$$w_{pr} = -|\Gamma_{ac}|/2\pi b' \quad (7)$$

where Γ_{ac} is the centerline circulation bound in the wing, which is the same as the magnitude of the total circulation in each of the two vortices in the pair. The magnitude of the downward velocity varies from one ft/s (1/3 m/s) for small aircraft to about 10 ft/s (3.05 m/s) for large heavily-loaded aircraft. When the wake-generating aircraft is within about one wing span or less above the ground, the self-induced downward velocity of the vortex pair turns more and more into a lateral velocity so that the spacing between the two vortices becomes larger with time when the vortices are near the ground plane. The maximum value for the lateral velocity occurs when wheel contact is made with the ground. The subsequent self-induced lateral velocity of each vortex adds to the wake-spreading process and must be included in any computation used to determine wake-intrusion time.

As the wake decomposes and spreads when out of ground affect, its shape can often be approximated by an elliptically-shaped region. The downward velocity of the wake under those circumstances may then be estimated by a theory based on the downward momentum induced in the wake by the lift force.¹⁷ Therefore, if a value for wake breadth is available from observations³⁹ or from theoretical estimates, the downward velocity during wake decomposition and spreading is roughly given by

$$w_{decomp}(t) \approx w_{pr} [B_{oval}/B_{decomp}(t)]^2 \quad (8)$$

where, $B_{oval} \approx 2.08 b'/4$ is the initial breadth of the oval-shaped wake, which is usually in a horizontal orientation. The quantity $B_{decomp}(t)$ is the breadth of the decomposing wake (independent of whether its vertical or horizontal extent is largest). Eq. (8) indicates that as vortex wakes age their breadth best represents the downward momentum in the wake due to lift on the wake-generating wing. Therefore, as the wake spreads laterally, its descent velocity rapidly becomes smaller, and its affect on wake spreading decreases.

E. Long-Term Self-Induced Spreading by Turbulence.

After the long-wave instability reaches its maximum amplitude, the wake continues to spread as a function of the square-root of time due to residual turbulence in the wake itself. In Fig. 3, the locations where linking and loop formation begin, and where the maximum wave amplitude occurs, are indicated. After maximum amplitude occurs (at about $\tau = 43$), the wake continues to spread as the square root of time as part of its decay process.³⁹ As a result, the size of the wake-hazardous region continues to increase with time from its initial value due to turbulence, and due to the self-induced velocity field of the long-wave instability of a vortex pair. An empirical relationship for the spreading rate that follows maximum amplitude is now discussed, because long-term avoidance predictions are sometimes needed. The equation discussed was found from observations made of the condensation trails behind aircraft at cruise altitudes.³⁹ It predicts that, after the long-wave instability has gone to maximum amplitude, the lateral and vertical size of the hazardous region are given by

$$B_{hz}(t) \approx D_{hz} \approx b_g C_{hz} (\Delta t)^{1/2} \quad (9)$$

where, $C_{hz} \approx 0.5$. If no other wake-spreading processes are included in the analysis, the time begins when the wake is generated so that Δt is the time interval in seconds between the generation of the wake and the arrival of a following aircraft at the same along-trail station. Because Eq. (9) predicts values for the hazardous region that are too small when Δt is small, the breadth and depth of the wake-hazardous region remains constant at its initial value until the size predicted by Eq. (9) predicts a larger value (Fig. 3). At that time, Eq. (9) is used to predict the location of the outer boundary of the hazardous region. Because Eq. (9) is not an exact function of the dimensionless parameters used in this paper for the time/distance axis being used, the velocity of the aircraft, U_∞ , is assumed to be 200 ft/s in Fig. 3, and the span of the aircraft is assumed to be 200 ft, so that the time parameter is equivalent to seconds, or wingspans downstream of the station where the wake was generated.

When all of the contributions to wake spreading are included as shown in Fig. 3, the $(\Delta t)^{1/2}$ function given by Eq. (9) applies only after the long-wave instability has reached its maximum amplitude. Because the $(\Delta t)^{1/2}$ function given by Eq. (9) is then rarely centered on the location of the wake-generating wing, a reference or bias time must be determined so that the predicted breadth of the hazardous region passes through the maximum amplitude point shown on the various figures, at the proper bias time determined so that the curves predicted by Eq. (9) (with a bias time) passes through the maximum amplitude location. The bias time is determined by modifying Eq. (9) to read

$$B_{hzmax} = 2y_{maxamp} = C_{hz} (t - t_{bias})^{1/2} b_g \quad (10)$$

where, for $b_f/b_g \leq 0.5$, $B_{hz0} = 2.0$ so that $y_{maxamp}/b_g = 1.0 + \pi/2$ is the maximum amount of wake spreading brought about on each side of the wake centerline by the long-wave instability, at the dimensionless time, τ_{maxamp} . The time is converted to a time in seconds for a specific aircraft for b_g , and a flight velocity for U_∞ , by use of the relationship, $t = \tau b_g/U_\infty$. Eq. (10) passes through the maximum amplitude point when the bias time is given by

$$t_{bias} = \tau_{bias} b_g/U_\infty = t_{maxamp} - (2 y_{maxamp}/b_g C_{hz})^2 \quad (11)$$

By use of Eqs. (10) and (11), the final stage of wake spreading can be extended in Fig. (3) from the maximum amplitude point downstream to as far as needed.

F. Movement of Wake-Hazardous Boundaries by Wind and Gusts.

An aircraft on approach to a set of parallel runways behind a leading aircraft requires a vortex-free flight path along its entire approach path. Therefore, any wind or local gust velocity can cause the locations of vortex segments to move and spread relative to the flight path of the wake-generating aircraft. In this way, the movement and spread of the hazardous region is monitored for an estimate of the size of the safe zone illustrated in Fig. A6. discussed previously, it is assumed that the horizontal across-runway components of the wind, and their variations with time or gusts, are obtained along the flight path used by each wake-generating aircraft by use of either ground-based or instrumentation on-board the wake-generating aircraft. In Fig. 6, the upper case letters denote the time-averaged values for the wind components, and the lower case letters denote the maximum unsteady or gust magnitudes in these measurements. Also shown is the self-induced downward velocity of the wake. The motion and spread of wake-hazardous regions predicted by use of maximum measured values of the wind and gust velocities, is believed to be conservative, because, as mentioned previously, wind-tunnel observations of vortex meander indicate that vortex elements only move about 40% of the amount predicted by wind magnitude.¹⁹ Again, the difference between the two values needs to be studied by use of flight tests.

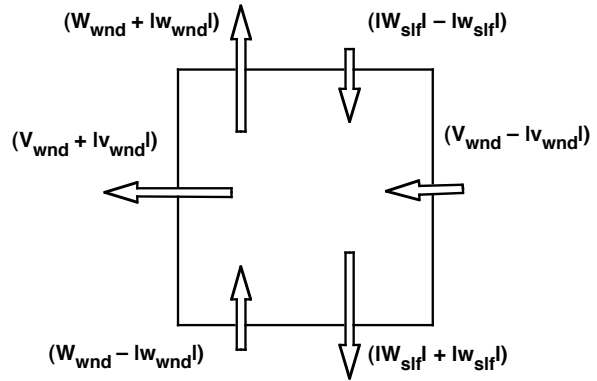


Fig. 6 Method used to move cross-sectional boundaries of wake-hazardous region in response to lateral and vertical wind and turbulence disturbance velocity components.

III. Estimate of Lateral Spreading Rate of Wake-Hazardous Region.

A. Equations for Wake Spreading.

The overall spread and motion of the wake-hazardous region at a given time or distance behind the wake-generating aircraft is determined by¹³⁻¹⁵

$$\Delta y_{\text{spread}} \approx B_{\text{hz}}(t)/2 + [V_{\text{ave}} + |V_{\text{err}}| + |w_{\text{pr}}|] \Delta t_{\text{ops}} \quad (12)$$

where Δy_{spread} is the amount that the wake-hazardous region has spread in the lateral direction at the time of arrival of a following aircraft. The quantity, $B_{\text{hz}}(t)$, is the amount that the wake-hazardous region has spread due to turbulence and the long-wave instability as a function of time. Because $B_{\text{hz}}(t)$ includes the wake-spreading amount caused by turbulence, the contribution brought about by the turbulence in the atmosphere is not entered a second time to the terms inside of the square brackets in Eq. (12). The parameter, Δt_{ops} , is the time difference between the arrival of the leading and following aircraft. The parameter, V_{ave} , represents the lateral velocity of movement of the wake or vortex elements caused by the time-averaged value of the wind component in the across-runway or y-direction. This term represents a choice that can often be made as to whether the following aircraft lands upwind or downwind of the preceding aircraft. When the flight path of the following aircraft can be specified as upwind of the flight path of the wake-generating aircraft, the sign of V_{ave} is negative. It can then contribute substantially to the reduction of the wake-spreading rate, and to an increase in the safe allowable along-trail separation distance between aircraft landing in a group. In this way, the time-averaged wind may be called a controllable quantity, because judicious arrangement of aircraft flight paths on approach can make it a beneficial or a detrimental quantity.

The quantity, $|V_{\text{err}}|$, is an estimate of the accuracy of the various wind and gust magnitudes as measured along the flight path of the wake-generating aircraft. Because measurements at small values are most sensitive to error, it is assumed that it has a value of 5 ft/s ($\approx 2\text{m/s}$). That amount is probably reasonable at low values of wind velocity, and may be conservative for larger wind magnitudes that are of most interest for wake avoidance. An absolute value is used for the $|V_{\text{err}}|$ quantity because it must be assumed to be random and will therefore always increase the magnitude of the total amount of wake spreading.

The quantity w_{pr} is always positive because the port and starboard vortices shed by an aircraft move in an outboard, horizontal direction from the flight path of the wake-generating aircraft when in ground effect. Therefore, the vortex shed by the leading aircraft that is closest to the flight path of the following aircraft always moves to spread the wake. The value of the sum of the lateral velocities in Eq. (12) is multiplied by, Δt_{ops} , to yield the total amount estimated for spreading of the wake of the leading aircraft laterally toward the flight path of the following aircraft.

The magnitude of the maximum gust velocity measured in any direction, $|V_{\text{gust}}|_{\text{max}}$, is used as an absolute value of the maximum value measured, because gusts can occur in any direction even though the largest magnitude measured along the flight path of the wake-generating aircraft might not have been in an unfavorable lateral direction. The contribution of $|V_{\text{gust}}|_{\text{max}}$ to wake spreading occurs in the determination of $B_{\text{hz}}(t)$ where it is used to determine the amount of spreading of the wake-hazardous region due to the long-wave instability as indicated by the last term in Eq. (6a).

The increase or decrease in wake spreading by an along-runway component of the wind is usually small, because the runway component of the wind simply shifts the wake components toward or away from the touchdown region of the runway surface. Although not included in Eq. (12), the offset in time experienced by vortex wakes when a wind of a significant magnitude is blowing as a head- or tail-wind along the approach path of the wake-generating aircraft has been included in the computer program listed in the Appendix. Examples calculated for an along-runway component of +10 or -10 ft/s predicted that an affect on wake-intrusion time above a second is not likely.

The equations for the lateral spread of the hazard posed by vortex wakes clearly indicate the benefits of short time intervals between aircraft operations. Firstly, short time intervals minimize the amount of time that the wind (and its uncertainties) have to move or spread the wake laterally. Secondly, short intervals of time also reduce the time available for the errors or omissions in wake movement and/or spreading to grow. Minimization of uncertainties makes it possible to operate more efficiently with greater latitude and safety on closely-spaced parallel runways, and to increase airport capacity by optimum amounts. Because of the significant number of parameters involved, it is recommended that the maximum allowable time difference before wake-intrusion occurs be determined by use of the computer program listed in the Appendix, or one like it.

B. Computer Program for Estimation of Wake Spreading.

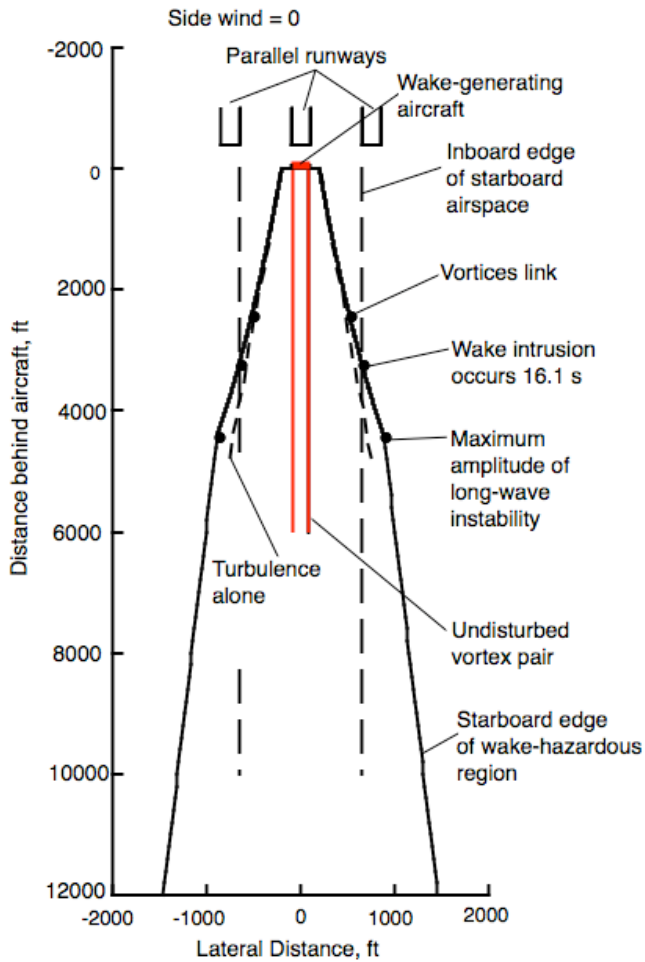
The large number of parameters that enter an estimate for the spreading of the wake-hazardous region as a function of time prompted the development of a computer program or code to expedite the computations needed, to

provide a graphical representation of wake-spreading in plan view, and to help prevent numerical errors from occurring (see Appendix). The computer program begins with the same program used to develop Fig. 3, which used dimensionless notation throughout. In the present code, the parameters are first converted from dimensionless notation to feet and seconds. In the figures presented, the same lines and their associated aerodynamic mechanism shown in Fig. 3 are presented in Figs. 7 and 8 to help orient readers as to the dynamics of the wake as it occurs. The resulting computer program is then set up to evaluate the wakes of various aircraft undergoing a variety of atmospheric and airport parameters. The atmospheric parameters used in the several examples shown in Figs. 7 and 8 include a zero magnitude and a 10 ft/s (3 m/s) side wind for an assumed atmospheric/wake turbulence level of 0.05. The along-runway wind component has been included in the computer program, but it has been set to zero in these figures because it usually has a negligible effect on wake-intrusion times. The two aircraft sizes studied are based on data for early versions of the B-747 and B-737, and may differ from more recent versions now in service.

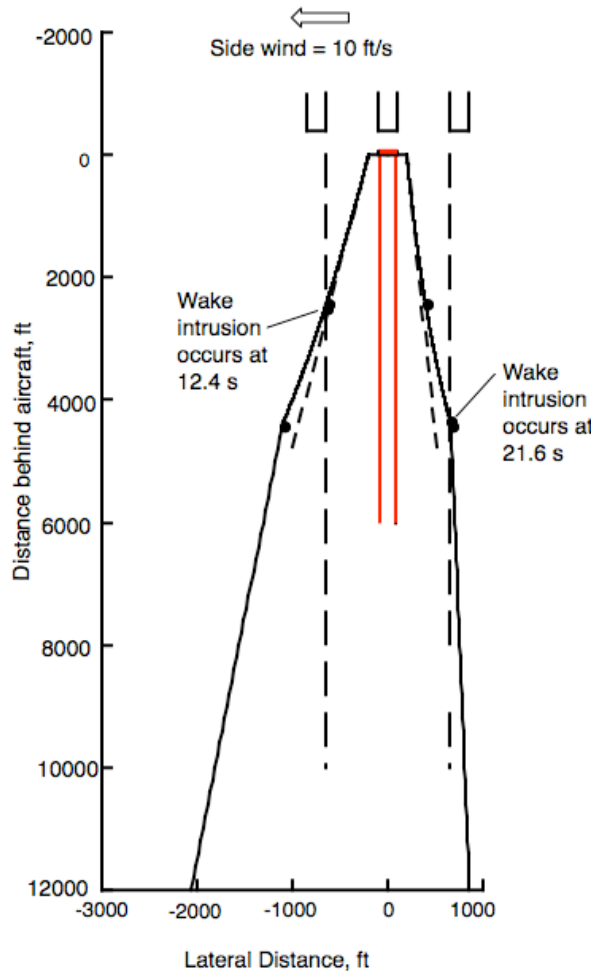
Both the upwind or windward and downwind or leeward boundaries of the wake-hazardous region are presented on the same figure to indicate the advantages achieved by having following aircraft land on runways upwind of the leading aircraft. The two different sizes of aircraft are used to illustrate the advantages achieved by having smaller aircraft land ahead of larger ones. The closely-spaced runways are assumed to be 200 ft (61 m) wide and to have 750 ft (229 m) between their centerlines. Large dots are placed at the locations where vortex linking and maximum amplitude events take place (as in Fig. 3), and where wake intrusion into the airspace of nearby runways is expected to occur—on either the up- or down-wind sides of the hazardous region posed by the leading aircraft. Distances behind the wake-generating aircraft are given in feet, and a representative number in terms of seconds is obtained by dividing distance by 200 ft/s (61 m/s), the flight velocity assumed for both the B-747 and the B-737. The computer program and the computations assume that the centerlines of the wake-generating and following aircraft never stray outside of the boundaries defined by the edges of the runway assigned to each of them. In other words, the computations consider only the aerodynamic part of wake avoidance.

Four examples are presented. Readers who may wish to include the techniques described here in their own research may consult the Appendix where a copy of the computer code is listed. The code presented is written in Fortran and was run on a G5 MacIntosh desk-top computer with each case taking only a few seconds to run.

In the cases presented, a corresponding estimate of the depth of the wake-hazardous region is not made because, although it varies from aircraft to aircraft, it is usually about the same as the magnitude estimated for the lateral spreading amount. Observations of condensation trails behind some aircraft at cruise indicate that the vertical spreading of vortex wakes may occur more rapidly than the lateral amount. It is assumed in the examples presented, and in the computer code, that the span-wise loading on the lifting surfaces of the aircraft is such that the vortex wake rolls up to form a single vortex pair, and that the entire circulation content on one side of the wing goes into the vortex and stays with it throughout the event. Because such an assumption is the most conservative, wake division is not considered.²⁰

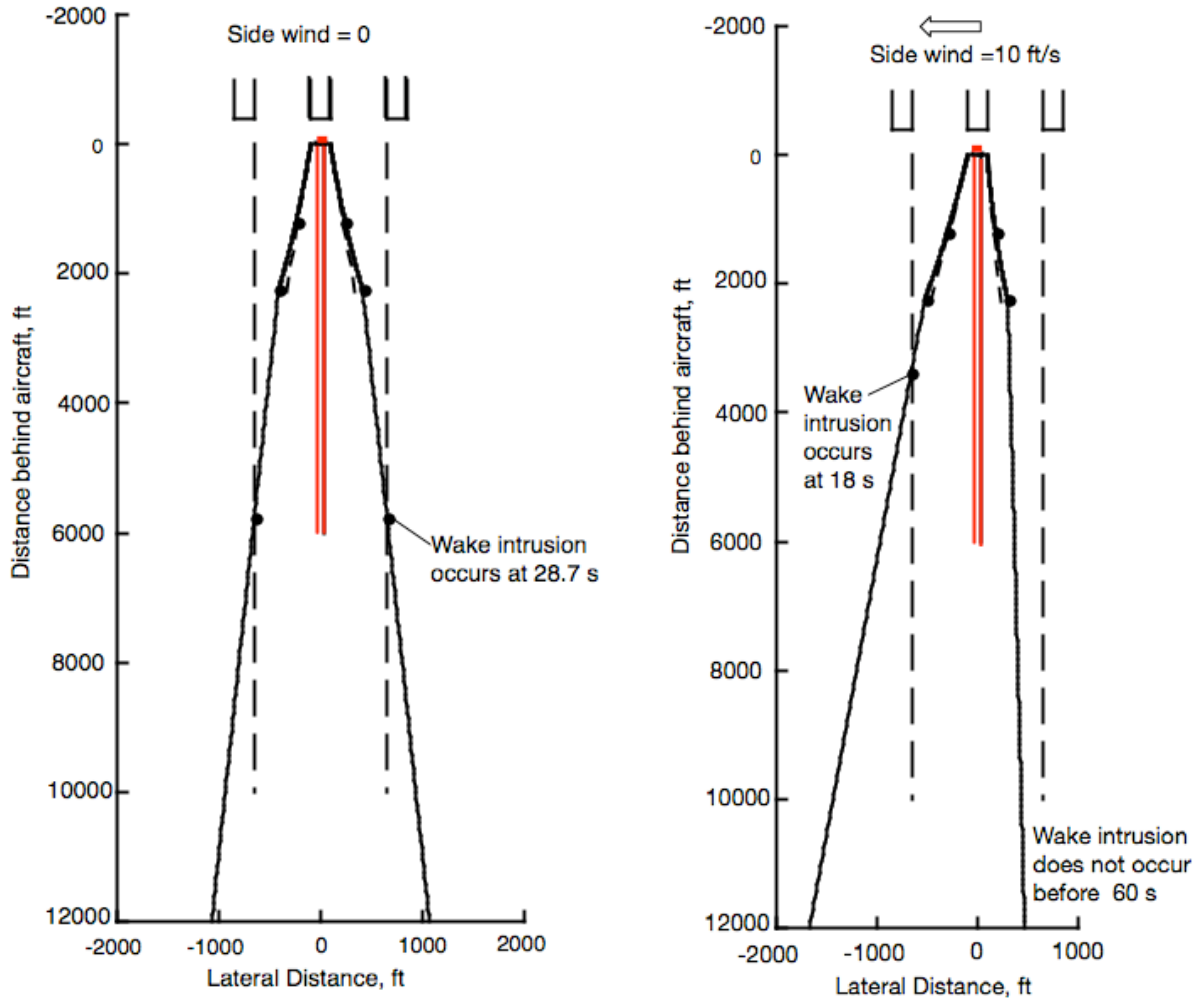


a. No side wind. Wake intrusion occurs at 3220 ft (16.1 s).



b. Side wind=10ft/s. Wake intrusion occurs at about 4320 ft (21.6 s) on windward side and at 2480 ft (12.4 s) on the leeward side of the wake.

Fig. 7 Plan view of components of wake-hazardous region shed by B-747 with numbered markers to indicate where various wake-spreading events take place. Computed by use of computer program listed in Appendix with $\epsilon_{eff} = 0.05$, and $V_{errfs} = 5$ ft/s. All other wind components are assumed to be of negligible magnitude.



a. No side wind, $\epsilon_{\text{eff}}=0.05$. Wake intrusion occurs at 5745 ft (28.7 s).

b. Side wind=10ft/s, $\epsilon_{\text{eff}}=0.05$. Wake intrusion occurs at 3375 ft (18 s) on leeward side, and after 12000 ft (60s) on windward side.

Fig. 8 Plan view of components of wake-hazardous region shed by B-737 with numbered markers to indicate where various wake-spreading events take place. Computed by use of computer program listed in Appendix with $\epsilon_{\text{eff}}=0.05$. and $V_{\text{errfs}}=5$ ft/s. All other wind components=0.

IV. Implications for Airport Operations.

The aerodynamic guidelines for efficiently avoiding vortex wakes of preceding aircraft are simple. The use of a computer program is recommended so that the large number of parameters that influence wake-intrusion time can be systematically included. If desired, it is may then be possible to add any of a number of non-aerodynamic parameters into the computer program to promote safety and an understanding of the disposition of aircraft and runway locations as a function of time. Because the duration of safe times before wake intrusion are on the order of a few tens of seconds, computer automation of advisory commands and decisions must be used for the determination of aircraft dispositions and guidance.

As far as how aircraft should efficiently avoid the hazard posed by vortex wakes, both intuition and the information presented in Figs. 7 and 8, point out that it is advisable to have following aircraft land upwind of

preceding aircraft because the side wind then blows wake components away from the flight path of following aircraft. It is also advisable to have smaller aircraft lead larger aircraft, because the cross sections of their wakes are correspondingly smaller, which tends to increase the time before wake intrusion occurs, and thus to promote safety. Additional safety is also achieved because larger aircraft can more easily tolerate the wake hazard caused by smaller aircraft. All following aircraft must, of course, comply with the estimates made for wake-intrusion times, and any non-aerodynamic or operational safety requirements advised for along-trail spacing of aircraft on approach to closely-spaced parallel runways at airports. The vertical depth or z-dimension of the wake-hazardous regions is not treated in detail, because it is recommended that all operations be carried out on a sloping planar basis wherein no aircraft ever travels above or below the flight path or active wake of another. It should be remembered that depth of wake-hazardous regions are about the same as their breadth, and wake components often extend above the flight path of the wake-generating aircraft.⁸ For these reasons, passage of aircraft above or below preceding aircraft should not be done until the wake has positively decomposed.

The foregoing text dealt with wake-avoidance considerations over only the regions where wake-intrusion might be a problem. The analysis and the computer program used to generate Figs. 7 and 8 dealt with the amount of spreading that occurs in vortex wakes as a function of time. Not analyzed is the time needed for the vortex wakes of an aircraft pair (or group) to decay to a harmless level, so that the airspace previously used is again safe to use; i. e., following aircraft must wait for the second safe region shown in Fig. 1. Called the aerodynamic recycle time for a given set of runways, it represents the time required for the hazard posed by all of the vortex wakes shed by the aircraft pair or group to decay to a harmless level, Δt_{dk} . The form of the computer program used to generate Figs. 7 and 8, and presented in the Appendix, needs a change in objective before it can be used to estimate the re-cycle time after a set of approaches and landings have been executed. That is, in its present form, the computations estimate the fastest rate at which the hazardous region posed by the wake will spread, and presumably decay. Therefore, the computation may also be used to estimate the shortest time interval required for the vortex wakes to decay to a harmless level. Safety requires, however, that the computation deliver an estimate of the longest time interval needed for the decay of the vortex wakes of both aircraft. Because the time interval required for the vortex wakes shed by leading aircraft to decay to a harmless level is uncertain, and difficult to estimate, the quantity Δt_{dk} should probably first be set at around three minutes, which is about one and one-half times as long than the longest waiting time now recommended. Flight tests are probably required to determine a more appropriate time interval.

A three-minute recycle time after each group of aircraft has landed offers the opportunity to intermittently utilize the set of closely-spaced parallel runways for arrival and departure of aircraft, and the crossing of active runways. It is reasoned that the wakes that trail from aircraft while on the ground and in a non-lifting situation consists only of turbulence, which becomes harmless within a few seconds after passage of the aircraft. Rapid decay occurs because the wakes of an aircraft on the ground do not contain lift-generated vortices that are highly coherent causing them to persist. That is, the intense highly coherent vortices present in wakes of aircraft while airborne are the elements that cause wakes to be hazardous and to persist. Because the wakes shed by aircraft while on a runway do not contain lift-generated vortices they decay to a non-hazardous level in 5s to 15s. As a result, almost the entire runway is vortex free during both arrival and departure of aircraft, thereby making it possible to recycle the use of the runway almost immediately after each set of operations. It is then possible to enhance the efficiency of airport operations by inter-lacing landing and take-off operations on runways. Air traffic controllers at airports appear to already be aware of such a traffic enhancement, because it is used frequently.

A large data sample of the locations of vortex centers has been obtained at the San Francisco International Airport by Hallock and Yang⁵⁰ for a wide variety of weather and wind conditions. It was found that vortex centers near the ground plane seldom move far enough in 30s to intrude into the airspace of an adjacent runway at 750 ft. However, their analysis did not account for the fact that the hazardous region extends almost half a wingspan outboard of the vortex centers. Therefore, the observations they made require a more complete estimation of the breadth of the hazardous region like the one utilized here before safety can be assured for 30 s time intervals for along-trail increments. If, however, the flight path of the two aircraft is restricted to those situations where a small aircraft is the lead aircraft, and where a side wind is blowing at about 10 ft/s or more, the foregoing guidelines indicate that the desired 30 s interval may safely be available on a nearly continuous basis.

V. Conclusions

A method is presented, along with a computer program, for estimation of the plan-form shape of the outer boundaries of the region where all of the hazardous elements of lift-generated vortex wakes are within to a high degree of certainty. The program appears to reliably predict the amount of along-trail distance or time between

arriving aircraft before the wake of a leading aircraft intrudes into the airspace of a following aircraft for operations on closely-spaced parallel runways. The examples presented indicate two simple rules. First, following aircraft should land upwind of leading aircraft, and secondly, smaller aircraft should precede larger aircraft. The reliability of the predictions for wake-intrusion time depends on how well the components of the time-averaged wind, its gust magnitudes, and the turbulence level along the flight path of each wake-generating aircraft can be measured for an accurate representation of wake spreading as a function of time.

The formulation proposed may be overly conservative, because three assumptions made to simplify the method for prediction of the spread of wake-hazardous regions. The first simplification is an assumption that the total circulation in each vortex is the maximum possible, so that the growth rate of the long-wave instability is based on the assumption that the wake contains a single vortex pair of the same strength as initially shed. The second simplification assumes that vortex elements travel with the wind and its larger disturbances without slippage or inertia. This conflicts with observations in wind tunnel tests that show that vortex segments move at about 40% of the disturbance velocities. The third assumption simplifies the measurement of turbulence (or flow field disturbances) in the atmosphere to a measurement of the maximum velocity observed in turbulent eddies within the wave-length or frequency range where the long-wave instability is initiated. Because these disturbances have a duration of several tens of seconds, they are referred to as gusts rather than turbulent velocity perturbations. As mentioned previously, the analysis has a non-conservative feature in that it was assumed that any un-planned motions of the wake-generating aircraft can be ignored in the computation of the amplitude of wake spreading. Because such motions by an aircraft are unplanned, inclusion in any prediction is difficult.

Because avoiding vortex wakes is a complicated safety concern, and uncertainties exist in the analysis and measurements taken, it is recommended that flight experiments be conducted to better define and confirm the theoretical models being suggested for use in the estimation of the spread of vortex wakes, and the wake-intrusion times that result. The flight experiments should also include measurements of the time required for the decay of the wakes of multiple aircraft in order to better estimate the recycle time for runway systems. The computational method presented is tailored for approach to runways, but the wake-avoidance features analyzed also apply to take-off situations.

Appendix. Computer Code for Wake-Spreading Estimates.

It should be noted that the copying process changes the indentation of the various lines of code, and that adjustments may need to be made when the following computer code is copied and pasted onto another computer.

```

Program W74703
c      AF VERNON J. ROSSOW-           April 10, 2008.
c      MAIN PROGRAM-----W74703.f/WkPlanView
c
c      THIS CODE DEVELOPED TO BE PART OF DISPLAY OF WAKE SPREADING AS A
c      FUNCTION OF TIME TO PROVIDE INFORMATION ON INTRUSION OF
c      WAKE-HAZARDOUS REGIONS INTO AIRSPACE OF A NEARBY PARALLEL RUNWAY.
c
c      Definitions:      alnk = SQRT(2) b'
c                       amax = 5.0*SQRT(2) b'
c                       Alnkbp= alnk/b' = Sqrt(2)
c                       Alnkgb= alnk/bg = Sqrt(2)*PI/4.0
c
c      Program assembles factors that cause wake-hazardous regions of
c      aircraft to move and spread as a function of time. The computer program
c      uses existing theories to estimate the various contributions for the
c      sides of the hazardous region so that it can be plotted in plan view to
c      display the port and starboard boundaries of the hazardous region as a
c      function of time or distance to better visualize how the various
c      contributions affect the along-trail safe zone for safety of operations
c      on closely-spaced parallel runways.
c
c      THIS PROGRAM SETS UP EQUATIONS FOR CALCULATION OF WAKE-SPREADING
c      AS A FUNCTION OF TIME TO ESTIMATE THE TIME AT WHICH THE
c      HAZARDOUS REGION POSED BY VORTEX WAKES WILL INTRUDE INTO THE
c      AIRSPACE OF A NEARBY CLOSELY-SPACED PARALLEL RUNWAY.

```

```

c     ALSO COMPUTES TIMES TO VORTEX LINKING, MAXIMUM AMPLITUDE OF LONG-WAVE
c     INSTABILITY AND THE AMPLITUDE OF WAKE SPREADING AS A FUNCTION OF TIME.
c
c     789012345678921234567893123456789412345678951234567896123456789712
c
c     COMMON BG,BGP,N(10),T(101),TT(101),AmplRa(101)
c     1,iout,Tadj(201)
c     2,Tau(4001),Ampbp(4001)
c     3,Ampbg(4001),xplt(20),yplt(20),F2(101)
c     4,Eef(101),TauLn(101),TauMx(101),TauLna(101),TauMxa(101)
c     5,dTauLn(101),dTauMx(101),Amplbp(101),Amplbg(101)
c
c
c     iout = 12
c     IF(iout.ne.6) open(UNIT=iout,FILE='W74703.out')
c
c     PI=ACOS(-1.0)
c     TWOPI=2.0*PI
c     FORPI=4.0*PI
c     PIHAF=PI*0.5
c
c     789012345678921234567893123456789412345678951234567896123456789712
c
c     WRITE(iout,1000)
c     1000 FORMAT(/,'AF VERNON J.ROSSOW  ','W74703.f      April 10, 2008  ')
c     WRITE(iout,1001)
c     1001 FORMAT(/,'STUDY OF AMPLITUDES OF LONG-WAVE INSTABILITY'
c     1,/, 'FOR IMPROVED PREDICTION OF WAKE-INTRUSION TIME'
c     2,/, 'and to calculate the time-history of growth of the long-wave'
c     3,/, 'instability of a vortex pair for display purposes.')
```

Parallel projection parameters:
THETZ= PI/3.0
THELV= PI/6.0
DYshft=0.0

```

c
c     BG   = WINGSPAN OF WAKE-GENERATING AIRCRAFT
c     BGP  = SPANWISE SEPARATION DISTANCE BETWEEN CENTERS OF VORTEX PAIR.
c
c     The computations that deal with the dynamics and growth of the
c     long-wave instability need to deal only with the amplitude of the waves
c     in the wave train as as given by a/bg' and the time as given by a
c     combination of circulation and time parameters that reduces to
c     t Gamma/bg'2. These non-dimensional results are then unscrambled so
c     that they can be applied to wake configurations that approximate the
c     dynamics of real wakes behind subsonic transport aircraft when the
c     atmosphere is turbulence and a side wind that is blowing across a
c     nearby runway to be used by a following aircraft.
c
c     The computations then indicate a time at which the spreading and moving
c     wake of the leading aircraft will intrude into the airspace soon to be
c     used by a following aircraft. This intrusion time dictates the maximum
c     length of time that the following aircraft can following the leading
c     aircraft; that is, the length of the safe zone.
c
c     Another code was set up to compute the Growth of Wave Amplitude as a
c     function of time for the Long-Wavelength Instability for Range of
c     Ambient Turbulence Levels. From this computation, several constants
```

```

c      were generated in order to form a close exponential match to the
c      numerically generated data. The two constants found are given by
c      C1 and C2. These two constants make it possible to calculate the
c      growth rate of the long-wave instability as a function of the
c      current amplitude of the instability. Determination of that derivative
c      makes it possible to calculate the growth of the instability as a
c      function of time. This explains the origin of the two constants used
c      to obtain the amplitude of the long-wave instability; namely
c      C1=0.16579
c      C2=0.04776
c
c      For turbulence only cases, Gam=0.0.
c
c      Iter=10
c      Npts=2000
c      Npts=3000
c
c      AIRCRAFT PARAMETERS for B-747
c      Bgft = 200.0
c      Ufts = 200.0
c      Sft2 = 5500.0
c      Wtlbs= 600000.00
c      Gam = 4.0*Wtlbs/(0.002378*PI*Ufts*Ufts*Bgft*Bgft)
c      If(Gam.LT.0.0001) Gam=0.0001
c      Wprfts = ABS(2.0*Gam*Ufts/(PI*PI))
c
c      WRITE(iout,1002) Bgft,Ufts,Sft2,Wtlbs,Gam,Wprfts
1002 Format(/,'AIRCRAFT PARAMETERS FOR B-747'
1,/, 'Bgft =',F8.2,' Ufts =',F8.2,' Sft2=',F8.2
2,/, 'Wtlbs=',F10.2
3,/, 'Gam=GamND =',F9.5,' Wprfts =',F9.5)
c
c      ATMOSPHERIC PARAMETERS AT AIRPORT
c      Uwndfs = 0.0
c      Vwndfs = 10.0
c      Wwndfs = 0.0
c      Vgstfs = 0.0
c      Vgstfs = 0.0
c      Eeff = Vgstfs/Ufts
c      Eeff = 0.01
c      VgstES = ABS(Vgstfs-Eeff*Ufts)
c      VgstES = 0.0
c      Verrfs = 5.0
c      VgstES is adjusted so that turbulence is not put in twice.
c      Uwndfs is along runway component of atmospheric wind
c      Vwndfs is across runway component of atmospheric wind
c      Wwndfs is vertical component of atmospheric wind--assumed to be zero
c
c      In order to prevent ridiculous gust levels from giving ridiculous
c      wake-intrusion times, a minimum value for Eeff is established at the
c      threshold measurement level. That is, the minimum is set at the
c      lower limit at which a wind velocity can be measured--at our current
c      ability to measure a wind velocity. That value is given by
c      Eeffmn = Verrfs/Ufts
c      If(Eeff.LT.Eeffmn) Write(iout, 1033) Eeffmn
c      If(Eeff.LT.Eeffmn) Eeff = Eeffmn
1033 Format(//,'ATMOSPHERIC TURBULENCE IS AT MINIMUM THAT CAN BE '
1, 'MEASURED',/, 'Eeff = Eeffmn =',F10.5)

```

```

c
c   VgstES is used in final spreading computations to prevent double
c   emphasis on same turbulence quantities that are present in the
c   atmosphere. The two quantities are being retained as two separate
c   measurements in case the measurement methods find that both Vgstfs and
c   Eeff are important for wake-spreading computations.
c   At this time its is believed that Vgstfs will always be larger than
Eeff.
c
c   789012345678921234567893123456789412345678951234567896123456789712
c
WRITE(iout,1003) Uwndfs,Vwndfs,Wwndfs,Vgstfs,VgstES,Verrfs,Eeff
1003 Format(/,'ATMOSPHERIC PARAMETERS AT AIRPORT'
1,/, 'Uwndfs =',F8.2,' Vwndfs =',F8.2,' Wwndfs =',F8.2
2,' Vgstfs=',F8.2,' VgstES=',F8.2
3,/, 'Verrfs =',F10.5,' Eeff =',F10.5
4,/, 'VgstES is adjusted so that turbulence is not put in twice')
c
c   PARAMETERS FOR AIRPORT SIZE,feet
RnwyBw = 200.0
RnwyCL = 750.0
c   Wake spreading distance to wake intrusion = RnwyCL - 0.5*RnwyBw =
WkIntD
WkIntD = RnwyCL - 0.5*RnwyBw
WRITE(iout,1004) RnwyBw,RnwyCL,WkIntD
1004 Format(/,'PARAMETERS FOR AIRPORT SIZE'
1,/, 'RnwyBw =',F8.2,/, 'RnwyCL =',F8.2,/, 'WkIntD =',F8.2)
c
c   Tau = dimensionless time = t(sec)*Ufts/Bgft
DTau=0.1
c
WRITE(iout,4108) Npts,Eeff,Gam,DTau
4108 Format(/,'Growth of wave amplitude is in diagonal direction until'
1,/, 'downstream distance specified is reached.'
2,/, 'Npts=',I4,' Eeff=',F9.5,' Gam=',F9.5
3,' DTau=',F9.5,/, ' J      K      Tau(k)  Ampbg(J,K) ')
Njump=-1
Do 41 K=1,Npts
Cay=K
Tau(K)=Cay*DTau
If(K.EQ.1) Tau(K)=0.0
If(K.EQ.1) Ampbg(K)=0.0
If(K.EQ.1) Go to 43
If(K.EQ.2) Ampbg(K)=1.0*Eeff*Tau(K)*Sqrt(2.0)
If(K.EQ.2) Go to 43
Ampbg(K)=Ampbg(K-1)+1.0*Eeff*DTau*Sqrt(2.0)
If(Ampbg(K).LT.0.1) Go to 43
Do 42 I=1,Iter
If(Iter.EQ.1) Ampave = (Ampbg(K)+Ampbg(K-1))*0.25
If(Iter.GT.1) Ampave = (Ampbg(K)+Ampbg(K-1))*0.5
DAMP1=0.16579*Gam*Ampave*((Alog(Ampave/0.04776))**(1.0/3.0))
DAMP2=+1.0*Eeff*Sqrt(2.0)
If(DAMP1.LT.0.0) DAMP=DAMP2
If(DAMP1.GT.0.0) DAMP=DAMP1+DAMP2
c   Because turbulence increases the spread on both sides of the wake.
c   The Sqrt(2.0) is needed because the turbulence spread is added to the
c   wave amplification, which is later divided by Sqrt(2.0).
c

```

```

c      789012345678921234567893123456789412345678951234567896123456789712
c
      Ampbg(K)=Ampbg(K-1)+DAmp*(Tau(K)-Tau(K-1))
42      Continue
43      Continue
c      Correction for b'/bg as adjustment to bg references.
      Bg = 1.0
      Bgp = Bg*PI/4.0
c      Linking occurs when a = Sqrt(2)*b'=Sqrt(2)*bg*PI/4.0
c      Max amplitude when a = 5*Sqrt(2)*b'=5*Sqrt(2)*bg*PI/4.0
c      Write(iout,4109) J,K,Tau(K),Ampbg(K)
c 4109 Format(2I5,8F10.5)
      If(Njump.GT.0.0) Go to 39
      If(Ampbg(K).GT.(0.5*2.0*Sqrt(2.0))*PI/4.0) TauLnk=Tau(K)
      If(Ampbg(K).GT.(0.5*2.0*Sqrt(2.0))*PI/4.0) AmpLnk=Ampbg(K)
      If(Ampbg(K).GT.(0.5*2.0*Sqrt(2.0))*PI/4.0) NLnk=K
      If(Ampbg(K).GT.(0.5*2.0*Sqrt(2.0))*PI/4.0) Njump=+1
39      Continue
c
      If(Ampbg(K).GT.(0.5*5.0*Sqrt(2.0))*PI/4.0) TauMax=Tau(K)
      If(Ampbg(K).GT.(0.5*5.0*Sqrt(2.0))*PI/4.0) AmpMax=Ampbg(K)
      If(Ampbg(K).GT.(0.5*5.0*Sqrt(2.0))*PI/4.0) NMax=K
      If(Ampbg(K).GT.(0.5*5.0*Sqrt(2.0))*PI/4.0) Go to 40
      NMax=K
41      Continue
40      Continue
      AmpMax=Ampbg(NMax)
      TauMax=Tau(NMax)
      Write(iout,4110) NLnk,TauLnk,AmpLnk,Eeff,NMax,TauMax,AmpMax
4110 Format('Diagonal amplitude of wave is large enough to link:'
1,/, 'NLnk=',I4, ' TauLnk=',F9.4, ' AmpLnk=',F9.4, ' Eeff=',F8.4
2,/, 'NMax=',I4, ' TauMax=',F9.4, ' AmpMax=',F9.4)
c
c      PREPARE DATA FOR FIRST PART OF HAZARDOUS BOUNDARY TO LINKING POINT.
      Bg=1.0
      Bgp=Bg*PI/4.0
      BfBg=0.5
c
c      789012345678921234567893123456789412345678951234567896123456789712
c
c      Analysis and computations from here on are again based on bg and
c      not b'.
c
      WRITE(iout,4111) Eeff,C3,C4,Bg,Bgp,BfBg,Gam,Bgft
4111 FORMAT(/,'Plan view of growth of Amplitude of Long-Wavelength '
1,'Instability ',/, 'Numerical Integration for '
2,'Time History (Dimensionless Notation):'
3,/, 'Eeff=',F9.4, ' C3=',F9.4, ' C4=',F9.4
4,/, 'Bg=',F9.4, ' Bgp=',F9.4, ' BfBg=',F9.4, ' Gam=',F9.4
5,/, 'Bgft=',F10.2
6,/, ' K Tau(K) BHZ BHZHf BHZHm'
7,/, ' DATA COMPUTED BUT NOT PRINTED OUT')
c
      If(BfBg.LE.0.5) BHZ0=2.0
      If(BfBg.GT.0.5) BHZ0=2.0+(BfBg-0.5)
      If(BfBg.GE.1.0) BHZ0=2.5
c      BHZ0 includes the initial spanwise spacing between vortex centroids
c      so that the factor +Bg*PI/4.0 does not need to be added onto BHZ.

```

```

      Do 45 K=1,NMax
      BHZ=BHZ0+2.0*Ampbg(K)/Sqrt(2.0)
      BHZHf=0.5*BHZ
      BHZHm=-BHZHf
      If(K.EQ.NLnk) BHZLnk=BHZHf
      If(K.EQ.NMax) BHZMax=BHZHf
c
c      WRITE(iout,4112) K,Tau(K),BHZ,BHZHf,BHZHm
c 4112 Format(I4,9F9.4)
      45 Continue
      44 Continue
c
      WRITE(iout,5110) NLnk,TauLnk,AmpLnk,NMax,TauMax,AmpMax
      1,Eeff
5110 Format(//,'NLnk=',I4,' TauLnk=',F9.4,' AmpLnk=',F9.4
      1,/, 'NMax=',I4,' TauMax=',F9.4,' AmpMax=',F9.4
      2,' Eeff=',F9.4)
c
c      789012345678921234567893123456789412345678951234567896123456789712
c
c      Prepare data for plots of FIRST part of edge of hazardous region
c      in terms of feet---that is from aircraft to maximum amplitude of
c      long-wave instability.
c
      WRITE(iout,4600)
4600 FORMAT(/,'Data in seconds and feet---'
      2,/, 'Plan View of Hazardous Region to Max Ampl'
      1,/, ' K Tsecs XStn YHZPrt YHZStr')
      IntP = -1
      IntS = -1
      K=0
      Tsecs=0
      XStn =0.0
      YHZPrt=0.0
      YHZStr=0.0
      WRITE(iout,4601) K,Tsecs,XStn,YHZPrt,YHZStr
      Do 46 K=1,NMax
      Tsecs = Tau(K)*Bgft/Ufts
      XStn = Tsecs*(Ufts+Uwndfs)
      BHZ=BHZ0+2.0*Ampbg(K)/Sqrt(2.0)
      YHZPrt=-0.5*BHZ*Bgft - (Vwndfs + VgstES + Verrfs + Wprfts)*Tsecs
      If(IntP.GT.0) Go to 461
      If(ABS(YHZPrt).GT.WkIntD) WkIntP = YHZPrt
      If(ABS(YHZPrt).GT.WkIntD) KIntP = K
      If(ABS(YHZPrt).GT.WkIntD) XStnP = XStn
      If(ABS(YHZPrt).GT.WkIntD) TsecsP = Tsecs
      If(ABS(YHZPrt).GT.WkIntD) IntP = +1
461 Continue
      YHZStr=+0.5*BHZ*Bgft + (-Vwndfs + VgstES + Verrfs + Wprfts)*Tsecs
      If(IntS.GT.0) Go to 462
      If(ABS(YHZStr).GT.WkIntD) WkIntS = YHZSTR
      If(ABS(YHZStr).GT.WkIntD) KIntS = K
      If(ABS(YHZStr).GT.WkIntD) XStnS = XStn
      If(ABS(YHZStr).GT.WkIntD) TsecsS = Tsecs
      If(ABS(YHZStr).GT.WkIntD) IntS = +1
462 Continue
      WRITE(iout,4601) K,Tsecs,XStn,YHZPrt,YHZStr
4601 Format(I5,4F10.2)

```

```

If(XStn.GT.12000.0) Go to 54
46 Continue
c
c Compute locations of linking and maximum point for long-wave instab.
c in feet and seconds for plots in real world.
c List data for where linking and maximum values occur in real world.
c
c 789012345678921234567893123456789412345678951234567896123456789712
c
c 789012345678921234567893123456789412345678951234567896123456789712
c
c PREPARE DATA FOR PART OF HAZARDOUS BOUNDARY THAT GOES FROM
c FROM LINKING POINT TO END OF OBSERVATION REGION BY USE OF
c Sqrt OF TIME FUNCTION; BHZ = 0.5 BG Sqrt(Adjusted time).
c
c Now extend outer edges of hazardous region further downstream from
c vortex linking point that was just computed. Assume that spreading is
c governed by activity of turbulence generated by aircraft and that
c its effectiveness depends only on its age. Therefore, use Tau values
c for time in the square root term. Do this for a B-747 on approach,
c because then Uinf/bg=1 sec, and Tau or Tac are in seconds or wingspans.
c Information on point of hazardous boundary to be extended is:
c NLnk,TauLnk,AmpLnk,Eeff
c
c BHZ0 includes the initial spanwise spacing between vortex centroids
c so that the factor +Bg*PI/4.0 does not need to be added onto BHZ.
c
c Taupse=Taupseudo=4.0*(BHZ0 + Sqrt(2.0)*AmpMax)**2
c Taupse= 4.0*(BHZ0 + 2.0*AmpMax/Sqrt(2.0))**2
c
c Convert dimensionless data to data in FEET for hazardous boundary
c from Max amplitude of instability to end of computational area.
c WRITE(iout,5111)
5111 FORMAT(/,'Growth of wake breadth after maximum amplitude '
1,/,', ' K Tsecs Xplot YHZEqP YHZEqS')

TauEnd=201.0
TauEnd=100.0
Nmxplt=NMax+200
Do 50 K=NMax,Nmxplt
Cay=K-NMax
Tplot=TauMax+Cay*1.0
Tsecs = Tplot*Bgft/Ufts
Xplot = Tsecs*(Ufts+Uwndfs)
Tac=Taupse+Cay*1.0
BHZ=0.5*Bg*Sqrt(Tac)
YHZPrt=-0.5*BHZ*Bgft - (Vwndfs + VgstES + Verrfs + Wprfts)*Tsecs
If(IntP.GT.0) Go to 4712
If(ABS(YHZPrt).GT.WkIntD) WkIntP = YHZPrt
If(ABS(YHZPrt).GT.WkIntD) KIntP = K
If(ABS(YHZPrt).GT.WkIntD) XStnP = Xplot
If(ABS(YHZPrt).GT.WkIntD) TsecsP = Tsecs
If(ABS(YHZPrt).GT.WkIntD) IntP = +1
4712 Continue
YHZStr=+0.5*BHZ*Bgft + (-Vwndfs + VgstES + Verrfs + Wprfts)*Tsecs
If(IntS.GT.0) Go to 4722
If(ABS(YHZStr).GT.WkIntD) WkIntS = YHZSTR
If(ABS(YHZStr).GT.WkIntD) KIntS = K

```



```

      If(ABS(YHZStr).GT.WkIntD) XStnS = Xplot
      If(ABS(YHZStr).GT.WkIntD) TsecsS = Tsecs
      If(ABS(YHZStr).GT.WkIntD) IntS = +1
4722 Continue
      WRITE(iout,5112) K,Tsecs,Xplot,YHZPrnt,YHZStr
5112 Format(I4,4F10.2)
      If(Xplot.GT.12000.0) Go to 54
50 Continue
54 Continue
c
c 789012345678921234567893123456789412345678951234567896123456789712
c
      WRITE(iout,4602)
4602 FORMAT(/,'Data in seconds and feet---'
1,/, 'Plan View of Points where Linking and Maximum Amplitudes'
2, ' occur',//, ' LkMx      Tsecs      XStnft      YHZPLk      YHZSLk')
      K = NLnk
      TLnk = Tau(K)*Bgft/Ufts
      BHZ=BHZ0+2.0*Ampbg(K)/Sqrt(2.0)
      YHZPLk=-0.5*BHZ*Bgft - (Vwndfs + VgstES + Verrfs + Wprfts)*TLnk
      YHZSLk=+0.5*BHZ*Bgft + (-Vwndfs + VgstES + Verrfs + Wprfts)*TLnk
      XStnLk = TLnk*(Ufts+Uwndfs)
      WRITE(iout,4603) K,TLnk,XStnLk,YHZPLk,YHZSLk
4603 Format(I5,4F10.2)
c
      K = NMax
      TMax = Tau(K)*Bgft/Ufts
      BHZ=BHZ0+2.0*Ampbg(K)/Sqrt(2.0)
      YHZPMx=-0.5*BHZ*Bgft - (Vwndfs + VgstES + Verrfs + Wprfts)*TMax
      YHZSMx=+0.5*BHZ*Bgft + (-Vwndfs + VgstES + Verrfs + Wprfts)*TMax
      XStnMx = TMax*(Ufts+Uwndfs)
      WRITE(iout,4604) K,TMax,XStnMx,YHZPMx,YHZSMx
4604 Format(I5,4F10.2)
c
      WRITE(iout,4612)
4612 FORMAT(/,'Data in secs and feet where Hazardous Region Intrudes'
1,/, 'Plan View of Points where Hazardous Region Intrudes'
2, ' occur',//, ' Kint      Tsecs      XInt      WkInt      ')
      If(IntP.GT.0) WRITE(iout,4601) KIntP,TsecsP,XStnP,WkIntP
      If(IntS.GT.0) WRITE(iout,4601) KIntS,TsecsS,XStnS,WkIntS
c
c
c 789012345678921234567893123456789412345678951234567896123456789712
c
      WRITE(iout,7001) BHZ0
7001 FORMAT(//,'BHZ0=',F10.2
1,/, 'Spread of Haz. region in FEET due to turbulence only '
2,//, ' J      Tsecs      Xplot      YTurBP      YTurbs')
c
      do 71 J=1,21
      Yay=J-1
      Tsecs = 2.0*Yay
      Xplot= Tsecs*(Ufts+Uwndfs)
      BHZ=BHZ0*Bgft+2.0*Eeff*Xplot
      YTurBP=-0.5*BHZ - (Vwndfs + VgstES + Verrfs + Wprfts)*Tsecs
      YTurbs=+0.5*BHZ + (-Vwndfs + VgstES + Verrfs + Wprfts)*Tsecs
      WRITE(iout,5112) J,Tsecs,Xplot,YTurBP,YTurbs
7002 Format(I4,9F10.2)

```

```

      If(Xplot.GT.XStnMx) Go to 72
71  Continue
72  Continue
c
c  End of data listing for plot of boundaries of hazardous region.
c
c  789012345678921234567893123456789412345678951234567896123456789712
c
c  Set up reference lines for wing and wake--in terms of FEET.
  Chord = 0.25*Bgft
  xplt(1) = 6000.0
  yplt(1) = -0.5*Bgft*(PI/4.0)
  xplt(2) = 0.0
  yplt(2) = -0.5*Bgft*(PI/4.0)
  xplt(3) = 0.0
  yplt(3) = +0.5*Bgft*(PI/4.0)
  xplt(4) = 6000.0
  yplt(4) = +0.5*Bgft*(PI/4.0)
  xplt(5) = 0.0
  yplt(5) = +0.5*Bgft*(PI/4.0)
c
  xplt(6) = 0.0
  yplt(6) = +0.5*Bgft
  xplt(7) = 0.0-Chord
  yplt(7) = +0.5*Bgft
  xplt(8) = 0.0-Chord
  yplt(8) = -0.5*Bgft
  xplt(9) = 0.0
  yplt(9) = -0.5*Bgft
c
c
  WRITE(iout,6001)
6001 FORMAT(/,'Reference lines for Wake and Wing Layout '
1,/,', ' J      xwnwk      ywnwk ')
  do 61 J=1,9
  WRITE(iout,6002) J,xplt(J),yplt(J)
6002 Format(I4,9F10.2)
61  Continue
c
c
c  Set up reference lines for three runways--in terms of FEET.
c  First runway:
  xplt(1) = -5.0*RnwyBw
  yplt(1) = -0.5*RnwyBw
  xplt(2) = -2.0*RnwyBw
  yplt(2) = -0.5*RnwyBw
  xplt(3) = -2.0*RnwyBw
  yplt(3) = +0.5*RnwyBw
  xplt(4) = -5.0*RnwyBw
  yplt(4) = +0.5*RnwyBw
c
  WRITE(iout,8001)
8001 FORMAT(/,'Reference lines for Runway for Wake-Gen Aircraft'
1,/,', ' J      xrnw1      yrnw1 ')
  do 81 J=1,4
  WRITE(iout,8002) J,xplt(J),yplt(J)
8002 Format(I4,9F10.2)
81  Continue

```

```

c
c   Port runway:
xplt(1) =-5.0*RnwyBw
yplt(1) =-0.5*RnwyBw - RnwyCL
xplt(2) =-2.0*RnwyBw
yplt(2) =-0.5*RnwyBw - RnwyCL
xplt(3) =-2.0*RnwyBw
yplt(3) =+0.5*RnwyBw - RnwyCL
xplt(4) =-5.0*RnwyBw
yplt(4) =+0.5*RnwyBw - RnwyCL
c
WRITE(iout,8003)
8003 FORMAT(/,'Reference lines for Runway on Port Side'
1,/,/, ' J      xrnw2      yrnw2  ')
do 82 J=1,4
WRITE(iout,8004) J,xplt(J),yplt(J)
8004 Format(I4,9F10.2)
82 Continue
c
c
c   Starboard runway:
xplt(1) =-5.0*RnwyBw
yplt(1) =-0.5*RnwyBw + RnwyCL
xplt(2) =-2.0*RnwyBw
yplt(2) =-0.5*RnwyBw + RnwyCL
xplt(3) =-2.0*RnwyBw
yplt(3) =+0.5*RnwyBw + RnwyCL
xplt(4) =-5.0*RnwyBw
yplt(4) =+0.5*RnwyBw + RnwyCL
c
WRITE(iout,8013)
8013 FORMAT(/,'Reference lines for Runway for Following Aircraft-feet'
1,/,/, ' J      xrnw3      yrnw3  ')
do 812 J=1,4
WRITE(iout,8014) J,xplt(J),yplt(J)
8014 Format(I4,9F10.2)
812 Continue
c   789012345678921234567893123456789412345678951234567896123456789712
c
c   Wake Intrusion Lines at Inner Side of Airspace for Following Aircraft:
c   Port side.
Xplt(1) = 0.0
Yplt(1) =-(RnwyCL-0.5*RnwyBw)
Xplt(2) = 50.0*Bgft
Yplt(2) =-(RnwyCL-0.5*RnwyBw)
c
WRITE(iout,8005)
8005 FORMAT(/,'Port Wake Intrusion Line for Following Aircraft-feet'
1,/,/, ' J      XintP      YintP  ')
do 83 J=1,2
WRITE(iout,8006) J,Xplt(J),Yplt(J)
8006 Format(I4,9F10.2)
83 Continue
c
c   Starboard side.
Xplt(1) = 0.0
Yplt(1) =+(RnwyCL-0.5*RnwyBw)
Xplt(2) = 50.0*Bgft

```

```

      Yplt(2) = +(RnwyCL-0.5*RnwyBw)
c
      WRITE(iout,8007)
8007 FORMAT(/,'Strbd Wake Intrusion Line for Following Aircraft-feet'
      1,/,', ' J      Xints      Yints ')
      do 84 J=1,2
      WRITE(iout,8006) J,Xplt(J),Yplt(J)
84 Continue
c      789012345678921234567893123456789412345678951234567896123456789712
c
c
      703 STOP
      END
c

```

VII. References

- ¹Rossow, V. J., "Lift-Generated Vortex Wakes of Subsonic Transport Aircraft," *Progress in Aerospace Sciences*, Vol. 35, No. 6, Aug. 1999, pp. 507-660.
- ²Spitzer, E. A., Hallock, J. N., and Wood, W. D., "Status of the Vortex Advisory System," *Proceedings of the Aircraft Wake Vortices Conference*, edited by J. N. Hallock, Report No. FAA-RD-77-68, U. S. Dept. of Transportation, March 15-17, 1977, pp 326-334.
- ³Hinton, D. A., "Aircraft Vortex Spacing System (AVOSS) Conceptual Design", *NASA TM 110184*, Hampton, VA, Aug. 1995.
- ⁴Rutishauser, D. K., and O'Connor, C. J., "Aircraft Wake Vortex Spacing System (AVOSS) Performance Update and Validation Study", *NASA/TM-2001-211240*, 2001.
- ⁵Burnham, D. C., Hallock, J. N., and Greene, G. C., "Increasing Airport Capacity with Modified IFR Approach Procedures for Close-Spaced Parallel Runways", *Air Traffic Control Quarterly*, Vol. 9, No. 1, 2001, pp. 45-58.
- ⁶Hallock, J. N., and Wang, F. Y., "Summary Results from Long-Term Wake-Turbulence Measurements at San Francisco International Airport", Report No. D0T-VNTSC-FA27-PM-04-13, *U. S. Dept. of Transportation*, Research and Special Programs Administration, Volpe National Transportation Systems Center, Aviation Safety Division, Cambridge, MA, July 2004.
- ⁷Hammer, J., "Case Study of Paired Approach Procedure to Closely Spaced Parallel Runways", *Air Traffic Control Quarterly*, Vol. 8, No. 3, 1999, pp. 223-252.
- ⁸High Approach Landing System / Dual Threshold Operation, developed by the German Air Safety Provider and Fraport, the Frankfurt Airport company. <http://www.dlr.de/ipa/>, and, <http://www.pa.op.dlr.de/wirbelschleppe>
- ⁹Koepp, F., "Doppler Lidar Investigation of Wake Vortex Transport Between Closely Spaced Parallel Runways", *AIAA Journal*, Vol. 32, No. 4, April 1994, pp. 805-810.
- ¹⁰Frech, M. , and Holzaepfel, F., "Skill of an Aircraft Wake-Vortex Model Using Weather Prediction and Observation". *AIAA Journal of Aircraft*, Vol. 45, No. 2, March-April 2008, pp. 461-470.
- ¹¹Rahm, S., Smalikho, I., and Koepp, F., "Characterization of Aircraft Wake Vortices by Airborne Coherent Doppler Lidar", *AIAA Journal of Aircraft*, Vol. 44, No. 3, May-June 2007, pp. 799-805.
- ¹²Rossow, V. J., "Wake-Vortex Separation Distances when Flight-Path Corridors are Constrained", *AIAA Journal of Aircraft*, Vol. 33, No. 3, May-June 1996, pages 539-546.
- ¹³Rossow, V. J., "Reduction of Uncertainties in Prediction of Wake-Vortex Locations", *AIAA Journal of Aircraft*, Vol. 39, No. 4, July-August 2002, pp. 587-596.
- ¹⁴Rossow, V. J., "Use of Individual Flight Corridors to Avoid Vortex Wakes", *AIAA Journal of Aircraft*, Vol. 40, No. 2, March-April 2003, pp. 225-231.

- ¹⁵Rossow, V. J., "Implementation of Individual Flight-Corridor Concept", AIAA-2003-6795, *AIAA 3rd Aviation, Technology, Integration, and Operations (ATIO) Forum – An Aviation System for the 2nd Century of Flight*, Denver, CO, Nov. 17-19, 2003.
- ¹⁶Rossow, V. J., Hardy, G. H., and Meyn, L. A., "Models of Wake-Vortex Spreading Mechanisms and Their Estimated Uncertainties", *AIAA 5th Aviation, Technology, Integration, and Operations (ATIO) Forum*, 26-28 Sept. 2005, Arlington, VA, AIAA 2005-7353.
- ¹⁷Rossow, V. J., "Classical Wing Theory and the Downward Velocity of Vortex Wakes", *AIAA Journal of Aircraft*, Vol. 43, No. 2, March-April 2006, pp. 381-385.
- ¹⁸Rossow, V. J., "Vortex-Free Flight Corridors for Aircraft Executing Compressed Landing Operations", *AIAA Journal of Aircraft*, Vol. 43, No. 5, Sept.-Oct. 2006, pp. 1424-1428.
- ¹⁹Rossow, V. J., and Meyn, L. A., "Relationship Between Vortex Meander and Ambient Turbulence", *AIAA 6th Aviation, Technology, Integration, and Operations (ATIO) Forum*, 25-27 Sept. 2006, Wichita, KS, AIAA 2006-7811.
- ²⁰Rossow, V. J., and Meyn, L. A., "On Data Scatter in Measured Linking Times for Lift-Generated Vortex Pairs", *46th AIAA Aerospace Sciences Meeting and Exhibit*, Reno, NV, January 7-10, 2008, AIAA-2008-0338.
- ²¹Holforty, W. L., and Powell, D. J., "Flight Deck Display of Airborne Traffic Wake Vortices", *20th Digital Avionics Systems Conference*, Daytona Beach, FL, Paper No. 154, Session 2A, Oct. 2001.
- ²²Hardy, G. H. and Lewis, E. K., "A Cockpit Display of Traffic Information for Closely Spaced Parallel Approaches", AIAA-2004-5106, *AIAA Guidance, Navigation and Control Conference and Exhibit*, 16-19, Providence, RI, August 2004.
- ²³Moralez, E. III, Tucker, G. E., Hindson, W. S., Frost, C. R., and Hardy, G. H., "In-flight Assessment of a Pursuit Guidance Display Format for Manually Flown Precision Instrument Approaches", *American Helicopter Society 60th Annual Forum*, Baltimore, MD, June 7-10, 2004.
- ²⁴Powell, J. D., Jennings, C., and Holforty, W. L., "Use of ADS-B and Perspective Displays to Enhance Airport Capacity", *24th Digital Avionics Systems Conference*, Washington, D. C., Paper No. 154, Session 2A, 3 Nov. 2005.
- ²⁵Arkind, K. D., "Maximum Capacity Terminal Area Operations in 2022", AIAA 2003-6791, *AIAA 3rd Aviation, Technology, Integration, and Operations (ATIO) Forum – An Aviation System for the 2nd Century of Flight*, Denver, CO, Nov. 17-19, 2003.
- ²⁶Miller, M. E., and Dougherty, S. P. "Communication and the Future of Air Traffic Management", Paper No. 0-7803-8155-6/04, *2004 IEEE Aerospace Conference*, Big Sky Montana, March 6 -13, 2004.
- ²⁷Arkind, K. "Requirements for a Novel Terminal Area Capacity Enhancement Concept in 2022," *AIAA Guidance, Navigation, and Control Conference*, August 2004.
- ²⁸Miller, M.E. and Trott, G.A., "Effects of Future Traffic on the National Airspace System," *AIAA M&S Conference*, August 2004.
- ²⁹Miller, M.E and Dougherty S P. "Advanced Terminal Area Communications Link Requirements", *23rd Digital Avionics Systems Conference*, October 2004, St. Lake City, UT.
- ³⁰Miller, M.E., Dougherty, S., Stella, J., and Reddy, P. "CNS Requirements for Precision Flight in Advanced Terminal Airspace", *IEEE Aerospace Conference*, March 2005.
- ³¹Verma, S., Lozito, S., Trot, G., and Ballinger, D. (in press). Guidelines for Flight Deck Procedures for Very Closely Spaced Parallel Runway Approaches. *NASA Technical Paper*, NASA Ames Research Center.
- ³²Cheng, V. H. L., "Airport Surface Operation Collaborative Automation Concept, "Proceedings of the *AIAA Guidance, Navigation, and Control Conference*, Austin, TX, August 11-14, 2003, AIAA Paper 2003-5773.
- ³³Cheng, V. H. L., "Research Progress on an Automation Concept for Surface Operation with Time-Based Trajectories," *7th Integrated Communications, Navigation, and Surveillance (ICNS) Conference*, Herndon, VA, May 1-3, 2007.
- ³⁴Rossow, V. J., and Tinling, B. E., "Research on Aircraft/Vortex-Wake Interactions to Determine Acceptable Level of Wake Intensity", *AIAA Journal of Aircraft*, Vol. 25, No. 4, June 1988, pp. 481-492.
- ³⁵Rossow, V. J., Sacco, J. N., Askins, P. A., Bisbee, L. S., and Smith, S. M., "Measurements in 80- by 120-Foot Wind Tunnel of Hazard Posed by Lift-Generated Wakes", *AIAA Journal of Aircraft*, Vol. 32, No. 2, March/April 1995, pages 278-284.

- ³⁶Rossow, V. J., Fong, R. K., Wright, M. S., and Bisbee, L. S., "Vortex Wakes of Two Transports Measured in 80- by 120-Foot Wind Tunnel", *AIAA Journal of Aircraft*, Vol. 33, No. 2, March/April 1996, pages 399-406.
- ³⁷Rossow, V. J., "Validation of Vortex-Lattice Method for Loads on Wings in Lift-Generated Wakes", *AIAA Journal of Aircraft*, Vol. 32, No. 6, Nov./Dec. 1995, pp. 1254-1262.
- ³⁸Schlichting, H., *Boundary-Layer Theory*, McGraw-Hill Book Company, 1955, pp. 735-755.
- ³⁹Rossow, V. J., and James, K. D., "Overview of Wake-Vortex Hazards During Cruise", *AIAA Journal of Aircraft*, Vol. 37, No. 6, 2000, pp. 960-975.
- ⁴⁰Zell, P. T., and Flack, K., "Performance and Test Section Flow Characteristics of the National Full-Scale Aerodynamics Complex 40- by 80-Foot Wind Tunnel", *NASA TM 101065*, Feb. 1989.
- ⁴¹Zell, P. T., "Performance and Test Section Flow Characteristics of the National Full-Scale Aerodynamics Complex 80- by 120-Foot Wind Tunnel", *NASA TM 103920*, Jan. 1993.
- ⁴²Crow, S. C., "Stability Theory for a Pair of Trailing Vortices", *AIAA Journal*, Vol. 8, No. 12, Dec. 1970, pp 2172-9.
- ⁴³Crow, S. C., and Bate, E. R., Jr., "Lifespan of Trailing Vortices in a Turbulent Atmosphere", *AIAA Journal of Aircraft*, Vol. 13, No. 7, July 1976, pp 476-482.
- ⁴⁴Tombach, I. H., "Observations of Atmospheric Effects on Vortex Wake Behavior," *AIAA Journal of Aircraft*, Vol. 10, No. 11, Nov. 1973, pp. 641-647.
- ⁴⁵Hinze, J. O., *Turbulence, An Introduction to Its Mechanism and Theory*, McGraw-Hill Book Co., Inc., 1959, pp. 180-190.
- ⁴⁶Biswas, G., and Eswaran, V., *Turbulent Flows, Fundamentals, Experiments and Modeling*, Narosa Publishing House, New Delhi, India, 2002, pp. 44-58.
- ⁴⁷Department of Defense Handbook, *Flying Qualities of Piloted Aircraft*, MIL-STD-1797A, 28 June 1995, Appendix A, 4.9.2 Definition of atmospheric disturbance model form. Pp. 678-687.
- ⁴⁸Rossow, V. J., "Prospects for Destructive Self-Induced Interactions in a Vortex Pair", *AIAA Journal of Aircraft*, Vol. 24, No. 7, July 1987, pp. 433-440.
- ⁴⁹Sarpkaya, T., "New Model for Vortex Decay in the Atmosphere," *AIAA Journal of Aircraft*, Vol. 37, No. 1, Jan.Feb. 2000, pp. 53-61.
- ⁵⁰Hallock, J. N., and Wang, F. Y., "Summary Results from Long-Term Wake Turbulence Measurements at San Francisco International Airport," Report No. DOT-VNTSC-FA27-{M-04-13, *U. S. Dept. of Transportation, Volpe National Transportation Systems Center*, Cambridge, MA, July 2004.